Using Mass Spectrometry to Quantitate and Analyze Bioactive Small Molecules

BY

CYNTHIA GRIM
B.S., University of South Florida, 2017

THESIS

Submitted as partial fulfillment of the requirements
for the degree of Master of Science in Pharmacognosy
in the Graduate College of the
University of Illinois at Chicago, 2020

Chicago, Illinois

Defense Committee:

Laura Sanchez, Chair and Advisor

Joanna Burdette

Brian Murphy

CONTRIBUTION OF AUTHORS

Chapter 1 is adapted from a published review (Grim, C.M., Luu, G.T., Sanchez, L.M., *FEMS Microbiology Letters*, 2019, 366, (11), fnz135) of which CMG is a primary co-author. Sections included within the chapter were primarily authored by CMG, with intensive editing and advice from the other authors.

Chapters 2 and 3 represent work that has not yet been adapted into a manuscript at this time.

TABLE OF CONTENTS

TABLE OF CONTENTS (continued)

LIST OF TABLES

LIST OF FIGURES

LIST OF FIGURES (continued)

LIST OF ABBREVIATIONS

^{13}C	Carbon-13
ACN	Acetonitrile
AUC	Area under the curve
CHCA	alpha-cyano-4-hydroxycinnamic acid
DHB	2,5,-dihydrobenzoic acid
DMEM	Dulbecco's Modified Eagle Media
ESI	Electrospray ionization
GC	Gas chromatography
GMF	Grouse's Modified Media Freshwater
GNPS	Global natural products social molecular networking
HPLC	High performance liquid chromatography
IMS	Imaging mass spectrometry
ISP-2	International Streptomyces Project-2
IT	Ion trap
LC	Liquid chromatography
LOD	Limit of detection
m/z	mass to charge ratio

MALDI	Matrix-assisted laser desorption/ionization
MAN	Metabolite association network
MCX	Mixed-mode cation-exchange
MeOH	Methanol
MFA	Metabolite flux analysis
MRM	Multiple reaction monitoring
MS	Mass spectrometry
MS^1	First level mass spectrometry
MS^2	Tandem mass spectrometry
MS/MS	Tandem mass spectrometry
NAP	Network Annotation Propagation
NMR	Nuclear magnetic resonance
PBS	Phosphate buffered solution
QqQ	Triple quadrupole
rRNA	Ribosomal RNA
SNF	Simple Nutrient Media Freshwater + Fiber
SPE	Solid phase extraction

SRM	Single reaction monitoring
TFA	Trifluoroacetic acid
TOF	Time of flight mass analyzer
V	Volts

SUMMARY

Metabolomics is the study of small molecules in a biological system. Metabolomics encompasses a wide range of research questions, and therefore requires the use of varied workflows. Chapter 1 is an overall introduction to targeted and untargeted metabolomics, as well as what kinds of experiments fall under each category. The chapter also serves as an introduction to mass spectrometers in the context of their metabolomics applications.

Chapter 2 applies fundamental targeted metabolomics techniques to a multiple reaction monitoring assay of catecholamines in cell media to investigate the role of catecholamines as chemical signals in the primary metastasis of epithelial high grade serous ovarian cancer This chapter reviews the necessary components of a working assay, with a focus on optimizing sample preparation for translating from an untargeted experiment to a targeted assay.

Chapter 3 details the process of cultivating a unique mammalian-sourced microbial library through untargeted metabolomics coupled with bioinformatics tools. This chapter focuses on the initial steps involved with developing a microbial library for drug discovery, starting with environmental isolation. This resulted in selecting 37 strains for a drug discovery library from 273 bacterial and 50 fungal isolates through pseudotaxonomic diversity and metabolite diversity.

CHAPTER 1. INTRODUCTION TO MASS SPECTROMETRY BASED METABOLOMICS TECHNIQUES

Based on excerpts from Grim, CM; Luu, GT; Sanchez, LM, Staring into the void: demystifying microbial metabolomics, FEMS Microbiology Letters, 2019, 366, (11), fnz135, by permission of Oxford University Press

1.1 Introduction

Metabolites are small molecules that drive biological systems from ecological to single-cell scales, in single cellular and multicellular organisms alike. For example, small molecules can act as chemical communicators among a quorum of similar microbes[1,2]. Small molecules from nature have garnered attention as sources of novel antibiotics, cancer therapeutics, painkillers, and more[3]. In mammals, neurotransmitters are particularly small, some less than 200 Daltons, but have relevance in Parkinson's disease[4], ADHD (Attention-Deficit/Hyperactivity Disorder)[5], Alzheimer's disease[6], among other neurological disorders. One way of classifying these molecules is by sorting them by purpose within an organism. Metabolites required for the survival of an organism have been termed "primary metabolites", while metabolites that perform secondary tasks such as chemical defense against predators are termed "secondary metabolites".

Primary metabolism includes well understood biochemical pathways, such as glycolysis. Since the target metabolites are known, the study of primary metabolism is often targeted in nature. A targeted metabolomics experiment requires tracking metabolites with high specificity and sensitivity. The progression of a disease can often be monitored through the abundance of a biomarker in a patient's serum, urine, or blood. These experiments require the accurate measurement of the analyte despite a complex background at low, often times nanomolar concentrations. Mass spectrometry has thus far been a crucial tool in research laboratories for its ability to study complex mixtures[7].

The secondary metabolites of an organism are often repurposed for pharmaceuticals[3]. For example, since the discovery of penicillin researchers have isolated microbial chemical

defenses to use them as antibiotics[8]. However, in the search for new antibiotics, challenges arise in finding novel metabolites or the failure to identify “known unknowns” which has led to high rates of rediscovery. Researchers have traveled the globe to search challenging environments in the hope of finding uniquely adapted microbes that produce uncommon chemistry to survive in harsh conditions. However, researchers often still face a plethora of overlapping chemistry in the face of their attempts to diversify their microbial libraries. New mass spectrometry tools exist to help profile the metabolite production of microbes earlier in the process so that less money and time are spent re-discovering common bioactive molecules.

Metabolomics studies fall into different categories that dictate the ideal instrumentation and approach to achieve different research goals. Figure 1.1 shows a basic outline of how a researcher may choose the tools best suited for their research question. This chapter summarizes the cases for common mass spectrometry instrumentation and data analysis workflows. The following chapters will explore specific uses of these workflows to address both targeted and untargeted research questions.

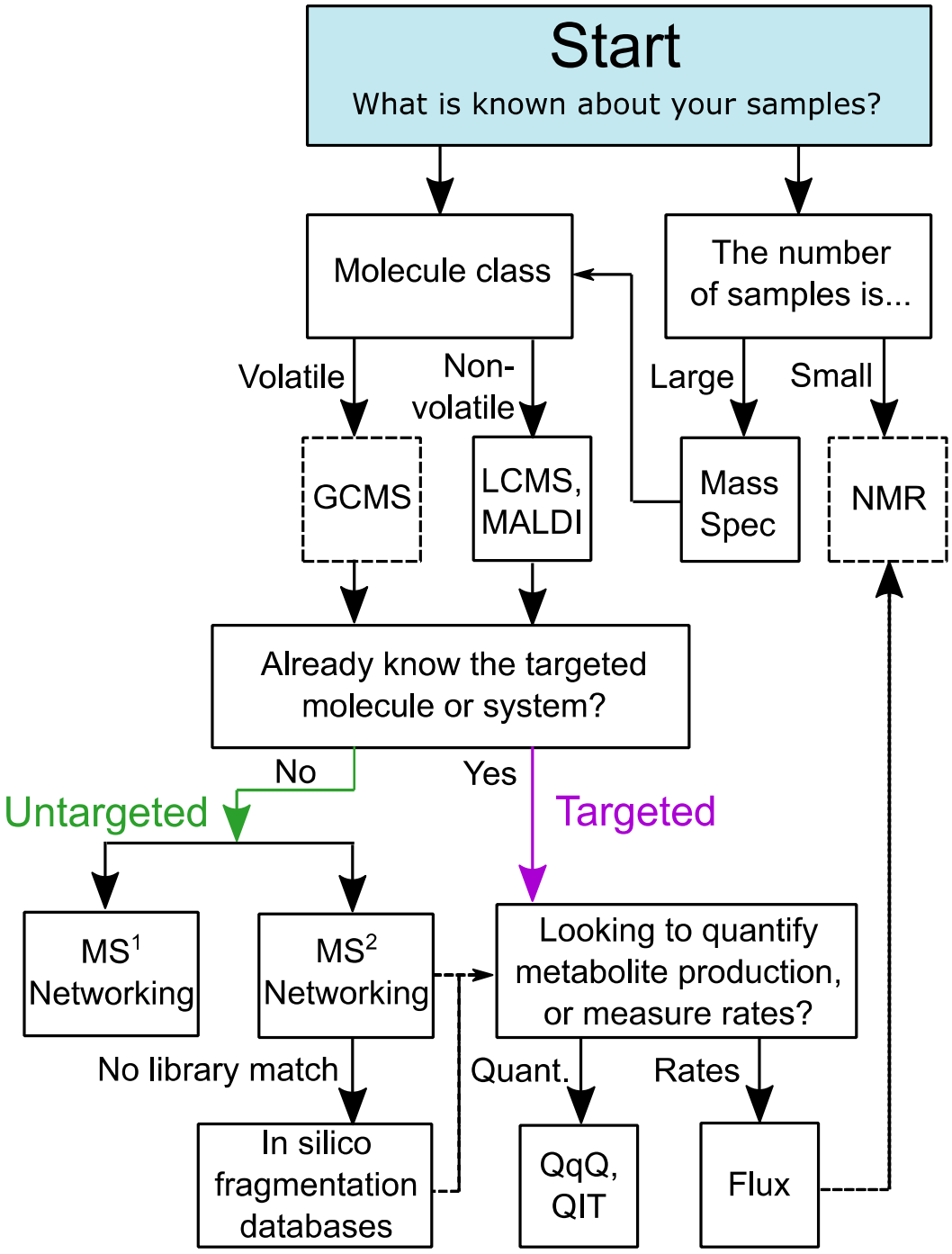

Figure 1.1. Workflow decision tree. Dashed lines indicate methods that are not covered in this chapter. Abbreviation key: GCMS (Gas chromatography mass spectrometry), LCMS (liquid chromatography mass spectrometry), MALDI (matrix assisted laser desorption/ionization), QqQ (triple quadrupole), QIT (quadrupole-ion trap)

1.2 Instrumentation

The use of analytical instrumentation is essential in the field of metabolomics. Nuclear magnetic resonance (NMR) and mass spectrometry (MS) can both be utilized in metabolomics, with MS typically being best suited for large sample sizes and cases requiring high sensitivity[9]. Mass spectrometry-based techniques detect ions, which can be either positively or negatively charged molecules that are denoted as mass to-charge ratios (*m/z*) each with a corresponding intensity value. Mass spectrometers operate under vacuum and require an ion source to deliver analytes to the mass analyzer and then the detector. The primary methods for introducing samples are by gas chromatography (GC) and liquid chromatography (LC). However, lasers can also be used to desorb ions from a solid phase such as in matrix-assisted laser desorption/ ionization (MALDI).

1.2.1 Chromatography

Chromatography helps separate analytes before introducing them to the ion source. This may help simplify what is being ionized simultaneously to increase sensitivity. Additionally, chromatography adds the dimension of time. Analytes spread out across a column based on their affinity to the stationary phase, such that compounds that are detected early on have very low affinity while compounds that elute late have a very high affinity. This often translates to information about an analyte's polarity.

GC-MS is best suited for volatile metabolites or those that can be derivatized as such. Ions in GC-MS are created via electron ionization, a form of hard ionization that produces molecular ions $[M]^{\cdot +}$. During ionization, metabolites fragment and are separated by the mass analyzer. This ability to fragment ions combined with high resolution, sensitivity,

reproducibility, and large compound libraries makes GC-MS the preferred instrument for analysis of volatile metabolites under 1000 Da[10]. However, the current limitations include the inability to analyze metabolites, especially unknowns, that don't fit those criteria, such as larger, non-volatile metabolites that are unable to be derivatized into volatile compounds. GC-MS is a robust and well understood form of mass spectrometry, but libraries and tools based on LC-MS are rapidly evolving to better understand the non-volatile chemical space.

Introducing liquid samples to the vacuum environment of a mass analyzer was made possible by the introduction of electrospray ionization (ESI). Electrospray ionization sprays a fine, charged mist of the analyte which causes the solvent to evaporate prior to introduction to the vacuum environment[11]. The ions are then able to proceed to the mass analyzer under vacuum. Most biomolecules are non-volatile and water soluble, so this was a major breakthrough for the field of metabolomics. Additionally, ESI is considered soft ionization. Analytes, including intact proteins, can be detected as ions of $[M+H]^+$ or $[M-H]^-$ instead of the rigorous fragmentation found in GC-EI-MS.

1.2.2 Mass Analyzers for Targeted and Untargeted Metabolomics

Targeted metabolomics analyzes the differences in a selected few, typically structurally characterized, metabolites. This can mean looking at the biotransformations a drug undergoes after it passes through the body in urine, or how much of a drug was present in the bloodstream of an individual. Untargeted metabolomics instead looks at all or a broad selection of metabolites in a system. A common example of untargeted metabolomics is in the development of an extract library. Extracts, often from environmental sources, are all stored to be tested against a variety of assays for bioactivity. Commonly these assays include the

extract's potential as a chemotherapeutic or an antibiotic. In an untargeted approach, it is unknown what single compound is causing the activity, but analytical chemistry can help determine if it's a known compound, what class it may fall under, or if it's completely unknown. Identifying if an experiment is untargeted or targeted is crucial in determining what mass analyzer is suitable for the experiment (Figure 1.1).

Targeted metabolomics generally looks to quantify the response of a system via a small selection of metabolites. This can be done as a relative measure, where the output would be that condition A elicits three times the response of condition B, or it can be done as an absolute measure. In absolute quantitation, the end result is a specific concentration of the analyte, such as 10 mM or 50 ng/L. Quantitative MS relies on tandem MS to filter and ensure the measurement of only the desired experimental analyte. The most common instrument for quantitative MS is the triple quadrupole, also known as the QqQ. Figure 1.2 shows a schematic depicting how ions travel through the three quadrupoles. First, a complex mixture of ions passes through the first quadrupole. By setting a fixed voltage on the poles, the quadrupole can effectively filter out all ions but ones that have the same *m/z* value as the analyte with unit specificity[12]. The second quadrupole introduces a neutral gas to fragment the precursor ions. The third quadrupole then again filters for a product ion that should be unique to the molecule of interest. This means that an ion was filtered at both the MS^1 and MS^2 level in order to be detected. This process is termed single reaction monitoring (SRM). Multiple reaction monitoring (MRM) involves the quadrupoles cycling through multiple set voltages to allow ions to pass through in sequence. The number of ions analyzed comes at the cost of sensitivity[13]. Quadrupole based instruments have been the longstanding instrument of choice in

quantitation because of the capability to filter ions and monitor individual *m/z* values with high sensitivity.

Untargeted experiments, by definition, do not have a molecule of interest to select and quantify in a given experiment. Hence, there is no specific ion or ion fragment that guides data collection. In this case, the mass analyzer used should be capable of collecting data across a wide array of *m/z* values. Generally, this means using time-of-flight (TOF), ion trap (IT), or orbitrap mass analyzers. Quadrupoles are frequently paired with TOFs and orbitraps, such as in the Q-Exactive, for high resolution and tandem data collection. Depending on the experiment, MS^1 or MS^2 data may be best suited for untargeted analysis.

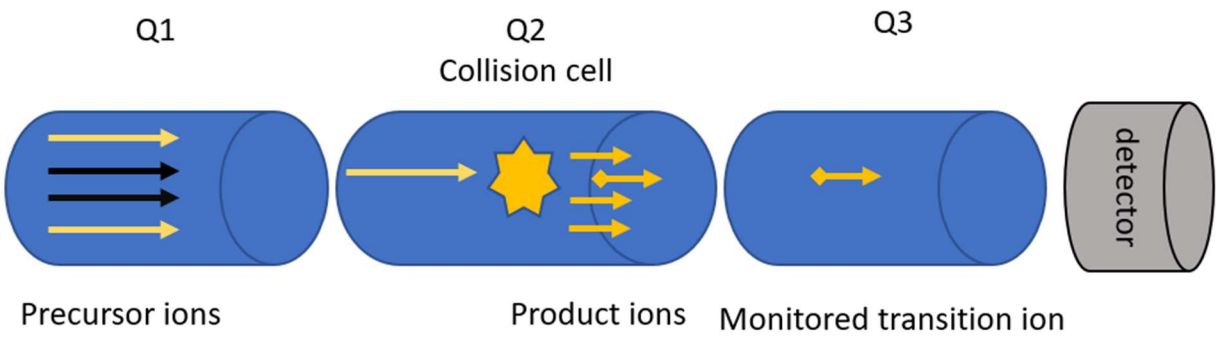

Figure 1.2 Diagram of SRM in a QqQ instruments. Black arrows represent ions that are not selected in the first quadrupole. The long yellow arrows represent ions that are selected in the first quadrupole. The short yellow arrows refer to product ions from the larger selected ion, and the short yellow arrow with the diamond node represents the ion selected in the third quadrupole.

1.3 Stable Isotope Approaches for Determining System Flux

Flux experiments involve using stable isotope labeled media to measure the rates of metabolic processes and exchange of metabolites in a living system[14]. While other metabolomics experiments focus on the presence, absence, or differences in metabolites, metabolite flux analysis (MFA) can determine the rate of metabolism and focuses heavily on primary metabolism and falls under the broad category of targeted metabolomics. In flux experiments, media with stable isotope labeled reagents are fed to cell cultures or whole organisms, which in turn ferment the reagents into amino acids and intracellular intermediates with the isotope atoms incorporated into their structure. For example, carbon-13 (^{13}C) is the most popular stable isotope for flux analysis labeling[15,16]. Deuterium is a frequent choice for other techniques requiring heavy labels, but deuterium is known to exchange with hydrogen readily and so is inappropriate for MFA. The location of the isotope on the metabolite's structure provides insight into what metabolic processes led to the formation of the metabolite. What becomes difficult is finding that specifically labeled atom in the structure, as a number of isotopologues can exist[14]. It is worth noting that elements have isotopes, whereas molecules have isotopologues for naming convention. Experiments have been designed to measure flux in colonies grown on solid agar[17], the effects of nutrition stress[18], and flux in co-culture[19]. Becker and Wittmann have thoroughly described a model MFA experiment using ^{13}C, GC-MS, and OpenFlux for *Corynebacterium glutamicum*, which provides step by step details on how a basic experiment was conducted[20].

GC-MS and MS^2 are both valid ways of conducting MFA analysis[20]. MS^2 is still being developed and implemented in standard fluxomic workflows, and so while it may be useful in coming years, it is not currently a standard workflow[21].

1.4 MS^1 Untargeted Prioritization

In GC and LC-MS, analytes are dissolved in a mobile phase and separated by a column before being introduced to the mass spectrometer. MALDI differs in that samples are introduced as co-crystalized solids. Additionally, LC-MS often gives rise to multiply charged species. Since a mass-to-charge ratio is a division of mass by charge, when looking at large proteins the *m/z* values that correspond to a protein of X Daltons can show up at approximately a third of X, a fourth of X, a fifth of X, and so forth. A MALDI-TOF-MS instrument can analyze molecules up to a very high molecular weight, and typically only produces singly charged species. This means that instead of a protein creating an abundance of multiply charged peaks, it might instead show a small selection of adducts. If the experiment calls for analyzing multiple proteins, MALDI-TOF-MS is generally recommended to avoid needing to deconvolute overlapping signals.

MS^1 networking has been used to identify bacteria based on their protein signatures with minimal sample preparation[22]. Ribosomal proteins are the most abundant in bacteria, and sequencing the 16S rRNA subunit is the standard identification technique to identify the genus and sometimes species of a bacterium. However, those abundant proteins can also be detected by MALDI-TOF-MS. Although the spectra cannot report a nucleic acid sequence, the spectra can be compared to databases of MALDI-TOF-MS spectra collected of known bacteria to find a match[23].

IDBac is an open source platform using the same principle[24,25]. After collecting protein data on a selection of microbes, the program uses similarity scoring on the protein spectra to organize strains in a pseudophylogenetic dendrogram. Additionally, MALDI-TOF-MS can collect MS^1 metabolite data from the same sample preparation. The nominal mass is limited in its ability to identify a metabolite, but IDBac creates metabolite association networks (MANs) to show which strains share metabolites with the same nominal mass. Users can use the protein and metabolite data together to choose strains they wish to further investigate. Some examples would be to select strains based on their putative taxonomic distance to known strains or their quantity of unique metabolite signals.

1.5 MS^2 Networking for Preliminary Compound Identification

MS^2 networking is a visualization tool that can be used to query the relationships between ions (metabolites) from any number of input files. The relationships are based on both the MS^1 and the product ions from the MS^2 spectrum. Relative and absolute mass differences and intensities between the products ions within a spectrum are compared across spectra to generate a cosine similarity score. The MS^2 spectra can be gathered in a number of ways from a cell culture including direct sampling of a developing microbial colony or by creating an extract from agar based colonies or fermentation broth[26]. This technique can, for example, identify molecules that may share a common core structure but have differing chemical modifications, such as additional amino acids, sugars, or different methylation patterns to name a few. This structural information is captured in an MS^2 spectrum as differences in mass, which indicate losses of chemical modifications that are shared across related metabolites. This workflow is very powerful because the database of “seed” metabolites is constantly growing allowing for

deeper annotation of metabolites from MS^2 datasets. A "seed" is the spectrum of a known metabolite that can be found in the GNPS (Global Natural Products Social molecular networking) database, or the spectrum of a metabolite from an in-house database; the terminology seed is meant to represent a known spectrum that can ground the unknown data to a known entity. GNPS also acts as a repository itself, where researchers can upload their own reference spectra to grow the knowledge base[27].

Microbiologists have already started using GNPS to identify metabolite group differences across different extraction conditions or different media types[28,29] . These experiments showed GNPS as a tool to identify major compound classes across many strains and conditions. Bauermeister *et al.* cultured six MAR4 *Streptomyces* strains and were able to compare metabolite production across strains as well as identify metabolite classes produced by the microbes. This led to a correlation of a cluster of novel ions with novel anti-biofilm activity[30].

It's worth noting that connectivity to a "seed" in a molecular network still requires validation rather than considering this a definitive identification. This is an important tool that can help generate hypotheses but should not be considered a standalone resource for identifications. The molecular network is only as good as the data collected and is also heavily reliant on the use of appropriate parameters when setting up the network.

1.5.1 *In silico* Databases Potentially Expand Known MS^2 Space

An important step in untargeted metabolomics experiments is the dereplication of 'known unknown' metabolites that are present among the hundreds/thousands in an extract. *In*

silico database searches have proven to be an invaluable technique towards this end. Through the use of databases such as Massbank[31], METLIN[32,33], GNPS[27,34,35], and more, MS^2 peak data can be used to annotate metabolites and provide putative structural information that was absent in MS^1 data. Despite its usefulness, *in silico* database searches are not absolute, and a compound's identity and structure must be experimentally verified using orthogonal methods such as MS^2 data, retention time, or NMR.

Although experimental data can provide the highest confidence in matching spectra to identify a metabolite, there is a bottleneck for how quickly an as of yet uncharacterized metabolites can be isolated, fragmented, and uploaded to repositories. *In silico* databases on the other hand have a high number of searchable spectra that may still match to a number of identified structures. Therefore, *in silico* databases are able to assist in metabolite dereplication. Compared to GC-MS, the number of LC-MS/MS spectra that have been curated is much smaller. To fill this gap, *in silico* fragmentation has been used to generate a greater number of mass spectra for comparison. METLIN has implemented *in silico* fragmentation simulations based on the spectra added to the database[36]. As of 2016, METLIN contained 240,000 molecules where 13,000 had experimental MS/MS data and there were 160,000 *in silico* fragmentation structure predictions[37].

While METLIN relies on the strength of their size of accumulated data to develop predictions, GNPS looks to improve confidence in fragmentation predictions through molecular networking. The Network Annotation Propagation tool (NAP) uses the fragmentation of neighboring nodes for the node in question to improve confidence in the structure prediction[35]. This feature is available through GNPS, but we recommend users familiarize themselves with

the basic molecular network techniques before attempting the experimental features. Additionally, since both of these tools are bolstered by the community's data, we encourage researchers to upload their own MS/MS data. Additionally, *in silico* fragmentation databases are compatible with any workflow that acquires MS/MS data. *In silico* databases and fragmentation have been more extensively covered in several recent reviews[38,39].

1.6 Conclusion

Mass spectrometry is a highly adaptable tool, well suited to both targeted and untargeted metabolomics. Specific instruments are often categorized by which branch they are best suited for, but bioinformaticians and analytical chemists have extended the applications of mass spectrometers through software development and experimental innovation.

The proceeding chapter describes the process of translating the sample preparation of an untargeted experiment incorporating a novel method of *in vitro* MALDI imaging mass spectrometry to a robust LC-MS/MS quantitation assay. The original method was designed to find chemical signals that were upregulated in a tumorigenic environment leading to metastasis in high grade serous ovarian cancer[40]. The MALDI-TOF-MS experiment was successful in generating a list of *m/z* values that were upregulated, however a targeted assay was necessary to further probe the context for the discovery. Despite the seemingly large divide between targeted and untargeted experiments, the two are still mutual partners within metabolomics.

The third chapter employs the use of bioinformatics tool IDBac to optimize a mammalian-sourced microbial drug discovery workflow. IDBac is an example of how a software can expand the uses for a specific MS instrument within the academic community, much like

how GNPS added a layer of information to MS/MS datasets. In this case, reducing the size of a drug discovery library while maintaining metabolite diversity is a cost-saving measure while employing the specific advantages of MALDI-TOF-MS. Chapter three demonstrates the amount by which a library can shrink as it is relevant to the research question.

1.7 Cited Literature

(1) Barnard, A. M. L.; Bowden, S. D.; Burr, T.; Coulthurst, S. J.; Monson, R. E.; Salmond, G. P. C. Quorum Sensing, Virulence and Secondary Metabolite Production in Plant Soft-Rotting Bacteria. *Philos. Trans. R. Soc. B Biol. Sci.* **2007**, *362* (1483), 1165–1183. https://doi.org/10.1098/rstb.2007.2042.

(2) Johnson, W. M.; Kido Soule, M. C.; Kujawinski, E. B. Evidence for Quorum Sensing and Differential Metabolite Production by a Marine Bacterium in Response to DMSP. *ISME J.* **2016**, *10* (9), 2304–2316. https://doi.org/10.1038/ismej.2016.6.

(3) Newman, D. J.; Cragg, G. M. Natural Products as Sources of New Drugs over the Nearly Four Decades from 01/1981 to 09/2019. *J. Nat. Prod.* **2020**, acs.jnatprod.9b01285. https://doi.org/10.1021/acs.jnatprod.9b01285.

(4) Dorszewska, J.; Prendecki, M.; Lianeri, M.; Kozubski, W. Molecular Effects of L-Dopa Therapy in Parkinson's Disease. *Curr. Genomics* **2014**, *15* (1), 11–17. https://doi.org/10.2174/1389202914666131210213042.

(5) Bowton, E.; Saunders, C.; Erreger, K.; Sakrikar, D.; Matthies, H. J.; Sen, N.; Jessen, T.; Colbran, R. J.; Caron, M. G.; Javitch, J. A.; Blakely, R. D.; Galli, A. Dysregulation of Dopamine Transporters via Dopamine D2 Autoreceptors Triggers Anomalous Dopamine

Efflux Associated with Attention-Deficit Hyperactivity Disorder. *J. Neurosci.* **2010**, *30* (17), 6048–6057. https://doi.org/10.1523/JNEUROSCI.5094-09.2010.

(6) Kandimalla, R.; Reddy, P. H. Therapeutics of Neurotransmitters in Alzheimer's Disease. *J. Alzheimers Dis.* **2017**, *57* (4), 1049–1069. https://doi.org/10.3233/JAD-161118.

(7) Jannetto, P. J.; Fitzgerald, R. L. Effective Use of Mass Spectrometry in the Clinical Laboratory. *Clin. Chem.* **2016**, *62* (1), 92–98. https://doi.org/10.1373/clinchem.2015.248146.

(8) American Chemical Society International Historic Chemical Landmarks. Discovery and Development of Penicillin http://www.acs.org/content/acs/en/education/whatischemistry/landmarks/flemingpenicillin.html (accessed Apr 1, 2020).

(9) Marshall, D.; Powers, R. Beyond the Paradigm: Combining Mass Spectrometry and Nuclear Magnetic Resonance for Metabolomics. *Prog. Nucl. Magn. Reson. Spectrosc.* **2017**, *100*, 1–16. https://doi.org/10.1016/j.pnmrs.2017.01.001.

(10) Rowan, D. D. Volatile Metabolites. *Metabolites* **2011**, *1* (1), 41–63.

(11) Yamashita, M.; Fenn, J. B. Electrospray Ion Source. Another Variation on the Free-Jet Theme. *J. Phys. Chem.* **1984**, *88* (20), 4451–4459. https://doi.org/10.1021/j150664a002.

(12) Sreekumar, J.; Hogan, T. J.; Taylor, S.; Turner, P.; Knott, C. A Quadrupole Mass Spectrometer for Resolution of Low Mass Isotopes. *J. Am. Soc. Mass Spectrom.* **2010**, *21* (8), 1364–1370. https://doi.org/10.1016/j.jasms.2010.03.041.

(13) Duncan, M.; Gale, P.; Yergey, A. *The Principles of Quantitative Mass Spectrometry*, 1st ed.; Rockpool Productions: Colorado, 2006.

(14) Dai, Z.; Locasale, J. W. Understanding Metabolism with Flux Analysis: From Theory to Application. *Metab Eng* **2017**, *43* (Pt B), 94–102.

(15) Antoniewicz, M. R. Methods and Advances in Metabolic Flux Analysis: A Mini-Review. *J Ind Microbiol Biotechnol* **2015**, *42* (3), 317–325.

(16) Antoniewicz, M. R. A Guide to 13C Metabolic Flux Analysis for the Cancer Biologist. *Exp. Mol. Med.* **2018**, *50* (4), 19. https://doi.org/10.1038/s12276-018-0060-y.

(17) Wolfsberg, E.; Long, C. P.; Antoniewicz, M. R. Metabolism in Dense Microbial Colonies: 13C Metabolic Flux Analysis of E. Coli Grown on Agar Identifies Two Distinct Cell Populations with Acetate Cross-Feeding. *Metab Eng* **2018**, *49*, 242–247.

(18) Ji, F.; Shen, Y.; Tang, L.; Cai, Z. Determination of Intracellular Metabolites Concentrations in Escherichia Coli under Nutrition Stress Using Liquid Chromatography-Tandem Mass Spectrometry. *Talanta* **2018**, *189*, 1–7.

(19) Gebreselassie, N. A.; Antoniewicz, M. R. *13 C-Metabolic Flux Analysis of Co-Cultures: A Novel Approach*; 2015; Vol. 31.

(20) Becker, J.; Wittmann, C. *GC-MS-Based 13C Metabolic Flux Analysis*; 2014.

(21) Choi, J.; Antoniewicz, M. R. Tandem Mass Spectrometry for 13C Metabolic Flux Analysis: Methods and Algorithms Based on EMU Framework. *Front Microbiol* **2019**, *10*, 31.

(22) Veen, S. Q. van; Claas, E. C. J.; Kuijper, E. J. High-Throughput Identification of Bacteria and Yeast by Matrix-Assisted Laser Desorption Ionization-Time of Flight Mass Spectrometry in Conventional Medical Microbiology Laboratories. *J. Clin. Microbiol.* **2010**, *48* (3), 900–907. https://doi.org/10.1128/JCM.02071-09.

(23) Cain, T. C.; Lubman, D. M.; Weber, W. J.; Vertes, A. Differentiation of Bacteria Using Protein Profiles from Matrix-Assisted Laser Desorption/Ionization Time-of-Flight Mass Spectrometry. *Rapid Commun. Mass Spectrom.* **1994**, *8* (12), 1026–1030. https://doi.org/10.1002/rcm.1290081224.

(24) Clark, C. M.; Costa, M. S.; Sanchez, L. M.; Murphy, B. T. Coupling MALDI-TOF Mass Spectrometry Protein and Specialized Metabolite Analyses to Rapidly Discriminate Bacterial Function. *Proc. Natl. Acad. Sci.* **2018**, *115* (19), 4981–4986. https://doi.org/10.1073/pnas.1801247115.

(25) Costa, M. S.; Clark, C. M.; Ómarsdóttir, S.; Sanchez, L. M.; Murphy, B. T. Minimizing Taxonomic and Natural Product Redundancy in Microbial Libraries Using MALDI-TOF MS and the Bioinformatics Pipeline IDBac. *J. Nat. Prod.* **2019**, *82* (8), 2167–2173. https://doi.org/10.1021/acs.jnatprod.9b00168.

(26) Yang, J. Y.; Sanchez, L. M.; Rath, C. M.; Liu, X.; Boudreau, P. D.; Bruns, N.; Glukhov, E.; Wodtke, A.; de Felicio, R.; Fenner, A.; Wong, W. R.; Linington, R. G.; Zhang, L.; Debonsi, H. M.; Gerwick, W. H.; Dorrestein, P. C. Molecular Networking as a Dereplication Strategy. *J Nat Prod* **2013**, *76* (9), 1686–1699.

(27) Wang, M.; Carver, J. J.; Phelan, V. V.; Sanchez, L. M.; Garg, N.; Peng, Y.; Nguyen, D. D.; Watrous, J.; Kapono, C. A.; Luzzatto-Knaan, T.; Porto, C.; Bouslimani, A.; Melnik, A. V.; Meehan, M. J.; Liu, W.-T.; Crüsemann, M.; Boudreau, P. D.; Esquenazi, E.; Sandoval-Calderón, M.; Kersten, R. D.; Pace, L. A.; Quinn, R. A.; Duncan, K. R.; Hsu, C.-C.; Floros, D. J.; Gavilan, R. G.; Kleigrewe, K.; Northen, T.; Dutton, R. J.; Parrot, D.; Carlson, E. E.; Aigle, B.; Michelsen, C. F.; Jelsbak, L.; Sohlenkamp, C.; Pevzner, P.; Edlund, A.; McLean, J.; Piel, J.; Murphy, B. T.; Gerwick, L.; Liaw, C.-C.; Yang, Y.-L.; Humpf, H.-U.; Maansson, M.; Keyzers, R. A.; Sims, A. C.; Johnson, A. R.; Sidebottom, A. M.; Sedio, B. E.; Klitgaard, A.; Larson, C. B.; P, C. A. B.; Torres-Mendoza, D.; Gonzalez, D. J.; Silva, D. B.; Marques, L. M.; Demarque, D. P.; Pociute, E.; O'Neill, E. C.; Briand, E.; Helfrich, E. J. N.; Granatosky, E. A.; Glukhov, E.; Ryffel, F.; Houson, H.; Mohimani, H.; Kharbush, J. J.; Zeng, Y.; Vorholt, J. A.; Kurita, K. L.; Charusanti, P.; McPhail, K. L.; Nielsen, K. F.; Vuong, L.; Elfeki, M.; Traxler, M.

F.; Engene, N.; Koyama, N.; Vining, O. B.; Baric, R.; Silva, R. R.; Mascuch, S. J.; Tomasi, S.; Jenkins, S.; Macherla, V.; Hoffman, T.; Agarwal, V.; Williams, P. G.; Dai, J.; Neupane, R.; Gurr, J.; Rodríguez, A. M. C.; Lamsa, A.; Zhang, C.; Dorrestein, K.; Duggan, B. M.; Almaliti, J.; Allard, P.-M.; Phapale, P.; Nothias, L.-F.; Alexandrov, T.; Litaudon, M.; Wolfender, J.-L.; Kyle, J. E.; Metz, T. O.; Peryea, T.; Nguyen, D.-T.; VanLeer, D.; Shinn, P.; Jadhav, A.; Müller, R.; Waters, K. M.; Shi, W.; Liu, X.; Zhang, L.; Knight, R.; Jensen, P. R.; Palsson, B. O.; Pogliano, K.; Linington, R. G.; Gutiérrez, M.; Lopes, N. P.; Gerwick, W. H.; Moore, B. S.; Dorrestein, P. C.; Bandeira, N. Sharing and Community Curation of Mass Spectrometry Data with Global Natural Products Social Molecular Networking. *Nat Biotechnol* **2016**, *34* (8), 828–837.

(28) Crusemann, M.; O'Neill, E. C.; Larson, C. B.; Melnik, A. V.; Floros, D. J.; da Silva, R. R.; Jensen, P. R.; Dorrestein, P. C.; Moore, B. S. Prioritizing Natural Product Diversity in a Collection of 146 Bacterial Strains Based on Growth and Extraction Protocols. *J Nat Prod* **2016**, *80* (3), 588–597.

(29) Papazian, S.; Parrot, D.; Burý\v sková, B.; Weinberger, F.; Tasdemir, D. Surface Chemical Defence of the Eelgrass Zostera Marina against Microbial Foulers. *Sci Rep* **2019**, *9* (1), 3323.

(30) Bauermeister, A.; Pereira, F.; Grilo, I. R.; Godinho, C. C.; Paulino, M.; Almeida, V.; Gobbo-Neto, L.; Prieto-Davó, A.; Sobral, R. G.; Lopes, N. P.; Gaudêncio, S. P. Intra-Clade

Metabolomic Profiling of MAR4 Streptomyces from the Macaronesia Atlantic Region Reveals a Source of Anti-Biofilm Metabolites. *Env. Microbiol* **2019**, *21* (3), 1099–1112.

(31) Horai, H.; Arita, M.; Kanaya, S.; Nihei, Y.; Ikeda, T.; Suwa, K.; Ojima, Y.; Tanaka, K.; Tanaka, S.; Aoshima, K.; Oda, Y.; Kakazu, Y.; Kusano, M.; Tohge, T.; Matsuda, F.; Sawada, Y.; Hirai, M. Y.; Nakanishi, H.; Ikeda, K.; Akimoto, N.; Maoka, T.; Takahashi, H.; Ara, T.; Sakurai, N.; Suzuki, H.; Shibata, D.; Neumann, S.; Iida, T.; Tanaka, K.; Funatsu, K.; Matsuura, F.; Soga, T.; Taguchi, R.; Saito, K.; Nishioka, T. MassBank: A Public Repository for Sharing Mass Spectral Data for Life Sciences. *J. Mass Spectrom.* **2010**, *45* (7), 703–714. https://doi.org/10.1002/jms.1777.

(32) Guijas, C.; Montenegro-Burke, J. R.; Domingo-Almenara, X.; Palermo, A.; Warth, B.; Hermann, G.; Koellensperger, G.; Huan, T.; Uritboonthai, W.; Aisporna, A. E.; Wolan, D. W.; Spilker, M. E.; Benton, H. P.; Siuzdak, G. METLIN: A Technology Platform for Identifying Knowns and Unknowns. *Anal Chem* **2018**, *90* (5), 3156–3164.

(33) Montenegro-Burke, J. R.; Guijas, C.; Siuzdak, G. METLIN: A Tandem Mass Spectral Library of Standards. *Methods Mol. Biol. Clifton NJ* **2020**, *2104*, 149–163. https://doi.org/10.1007/978-1-0716-0239-3_9.

(34) Nothias, L. F.; Petras, D.; Schmid, R.; Duehrkop, K.; Rainer, J.; Sarvepalli, A.; Protsyuk, I.; Ernst, M.; Tsugawa, H.; Fleischauer, M.; Aicheler, F.; Aksenov, A.; Alka, O.; Allard, P.-M.; Barsch, A.; Cachet, X.; Caraballo, M.; Da Silva, R.; Dang, T.; Garg, N.; Gauglitz, J. M.;

Gurevich, A.; Isaac, G.; Jarmusch, A. K.; Kamenik, Z.; Kang, K. B.; Kessler, N.; Koester, I.; Korf, A.; Le Gouellec, A.; Ludwig, M.; H, C. M.; McCall, L.-I.; McSayles, J.; Meyer, S.; Mohimani, H.; Morsy, M.; Moyne, O.; Neumann, S.; Neuweger, H.; Nguyen, N. H.; Esposito-Nothias, M.; Paolini, J.; Phelan, V.; Pluskal, T.; Quinn, R. A.; Rogers, S.; Shrestha, B.; Tripathi, A.; van der Hooft, J. J. J.; Vargas, F.; Witting, M.; Yang, H.; Zhang, Z.; Zubeil, F.; Kohlbacher, O.; Bocker, S.; Alexandrov, T.; Bandeira, N.; Wang, M.; Dorrestein, P. Feature-Based Molecular Networking in the GNPS Analysis Environment, 2019.

(35) da Silva, R. R.; Wang, M.; Nothias, L.-F.; van der Hooft, J. J. J.; Caraballo-Rodríguez, A. M.; Fox, E.; Balunas, M. J.; Klassen, J. L.; Lopes, N. P.; Dorrestein, P. C. Propagating Annotations of Molecular Networks Using in Silico Fragmentation. *PLoS Comput Biol* **2018**, *14* (4), e1006089.

(36) Domingo-Almenara, X.; Guijas, C.; Billings, E.; Montenegro-Burke, J. R.; Uritboonthai, W.; Aisporna, A. E.; Chen, E.; Benton, H. P.; Siuzdak, G. The METLIN Small Molecule Dataset for Machine Learning-Based Retention Time Prediction. *Nat. Commun.* **2019**, *10* (1), 5811. https://doi.org/10.1038/s41467-019-13680-7.

(37) Levin, N.; Salek, R. M.; Steinbeck, C. Chapter 11 - From Databases to Big Data. In *Metabolic Phenotyping in Personalized and Public Healthcare*; Holmes, E., Nicholson, J. K., Darzi, A. W., Lindon, J. C., Eds.; Academic Press: Boston, 2016; pp 317–331.

(38) Gil de la Fuente, A.; Grace Armitage, E.; Otero, A.; Barbas, C.; Godzien, J. Differentiating Signals to Make Biological Sense - A Guide through Databases for MS-Based Non-Targeted Metabolomics. *Electrophoresis* **2017**, *38* (18), 2242–2256.

(39) Blaženović, I.; Kind, T.; Ji, J.; Fiehn, O. Software Tools and Approaches for Compound Identification of LC-MS/MS Data in Metabolomics. *Metabolites* **2018**, *8* (2).

(40) Zink, K. E.; Dean, M.; Burdette, J. E.; Sanchez, L. M. Imaging Mass Spectrometry Reveals Crosstalk between the Fallopian Tube and the Ovary That Drives Primary Metastasis of Ovarian Cancer. *ACS Cent. Sci.* **2018**, *4* (10), 1360–1370. https://doi.org/10.1021/acscentsci.8b00405.

CHAPTER 2. ASSAY DESIGN FOR THE QUANTITATION OF CATECHOLAMINES IN AN *IN VITRO* HIGH GRADE SEROUS OVARIAN CANCER MODEL

2.1 Introduction

High grade serous ovarian cancer is both the most common and most deadly form of ovarian cancer.[1–4].. More than half of ovarian cancer cases are diagnosed after the tumor has already metastasized, which carries only a 29.2% 5-year survival rate[2]. A previous imaging mass spectrometry (IMS) experiment showed that norepinephrine (**2.1**) was secreted by a healthy murine ovary in the presence of murine tumorigenic oviductal epithelial cell line[5]. However, the study was untargeted and required adaptation to LC-MS/MS to move forward with exploring the catecholamine pathway with both sensitivity and efficiency. The goal of this project was to design an absolute quantitative mass spectrometry-based assay to measure norepinephrine and other catecholamine products from an *in vitro* model of the ovarian cancer microenvironment.

2.1.1 Primary Catecholamines

Norepinephrine belongs to a class of molecules called "primary catecholamines" along with epinephrine (**2.2**) and dopamine (**2.3**). The molecules all belong to the same biosynthetic pathway stemming from metabolism of tyrosine. Dopamine converts into norepinephrine, which converts into epinephrine[6–9]. An accumulation of norepinephrine within the tumorigenic system may be the result of a malfunction elsewhere within the pathway. Therefore, it was decided to monitor all three of the primary catecholamines in order to develop experiments to contextualize the initial observation.

2.1.2 MRM Quantitative Assays

A standard multiple reaction monitoring (MRM) quantitation assay is a relatively quick and sensitive method for analyzing *in vitro* samples. With a quantitative assay, it would be

possible to compare responses of catecholamines at different time points, different cell lines, or with the presence or absence of key enzymes or receptors within the pathway. Analyzing the cell media of tumorigenic cell lines is an effective way to analyze metabolic pathways without the greater interference of a whole organism[10].

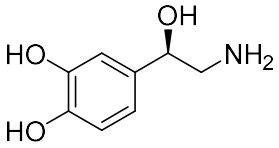

2.1

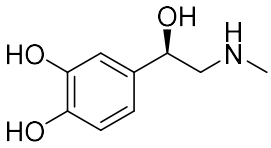

2.2

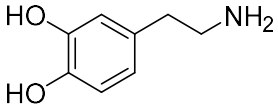

2.3

Figure 2.1 provides an overview of the sample preparation in a quantitation assay, as adapted from Duncan, Gale, and Yergey[11]. The first step is to generate calibration curve standards.

For absolute quantitation via mass spectrometry, internal standards are required[11]. The most common form of internal standard is a heavy (selectively deuterated) version of the analyte. Compounds **2.4-2.6** are heavy standards for the analysis of compounds **2.1-2.3** respectively. The internal standard behaves nearly identically to the analyte within the instrument, except it will register on the mass spectrometer with a *m/z* shift, allowing the response to be measured without overlapping signal from the analyte. Since the molecules are nearly identical, whatever perturbations in the system effect the response of the analyte will also similarly affect the response of the internal standard[11]. Since the concentration of the internal standard is the same across all samples, the ratio of the area under the curve (AUC) of

the heavy standard to the AUC of the light analyte acts as a normalized measurement of the analyte response.

2.1.3 Sample Preparation

The second step for the analysis of solid samples is to extract the analyte of interest so that it is dissolved in solvent compatible with liquid chromatography (LC) analysis. The internal standard must also be present in the extracts to aid in quantification. In the original *in vitro* model used by Zink *et al.*, cell culture media was mixed with low-melting agarose to fill an 8-well chamber slide[5], as depicted in **Error! Reference source not found.**. Each resulting well or "plug" represents one sample condition. The cell media used in this experiment is DMEM (Dulbecco's Modified Eagle Media). Since the media, and therefore the agarose wells, are water based, the analytes are capable of diffusing throughout the sample. Therefore, the internal standards will also diffuse through the sample. We have chosen to add the internal standards, norepinephrine-d_6 (**2.4**), epinephrine-d_6 (**2.5**), and dopamine-d_4 (**2.6**), to the wells before extraction to account for extraction efficiency and ionization efficiency simultaneously during data collection.

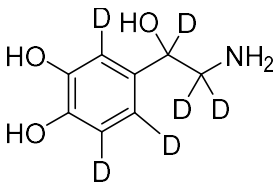

2.4

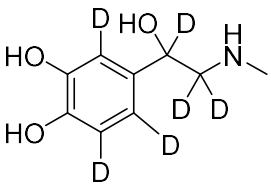

2.5

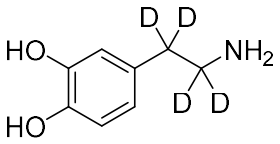

2.6

Generally, a targeted experiment involves measuring analytes within a complex mixture, such as blood, plasma, or urine. The biological fluid that carries the analyte is also called the

sample matrix. The matrix may contain proteins, cells, salts, or other compounds that reduce the ionization of the analytes and this reduction in ionization of the analytes is referred to as “matrix effect”. One way of reducing matrix effect is to use solid phase extraction (SPE). The SPE column works by the same principles of liquid chromatography. Analytes are retained by interactions with the solid phase to allow for separation from the sample matrix. When working with water or urine samples, there is often a high volume of matrix containing a very low concentration of analyte. Once again, an SPE column can help by accumulating retained analyte over the introduction of large volumes of sample, and then eluted in a small volume to concentrate the analyte. After sufficient “clean-up”, the samples are ready for introduction to the mass spectrometer either by chromatography or direct injection. Further information about instrumentation can be found in chapter 1, section 1.2.

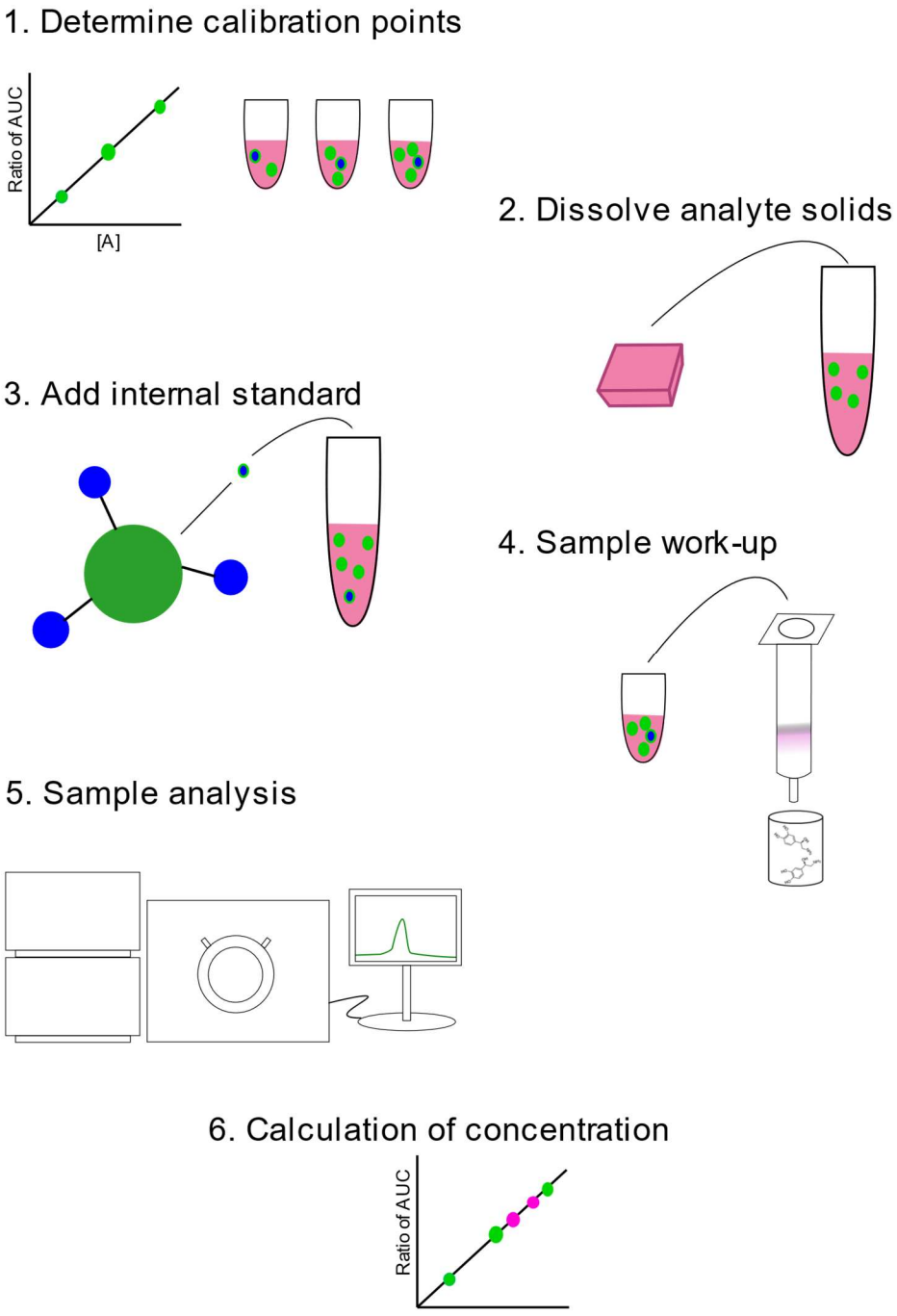

Figure 2.1. Quantitation basic workflow[11]. In this assay, an internal standard is added (step 3) before the analyte solids are dissolved (step 2). Green represents the analyte, and blue represents deuterium. Pink represents the sample matrix.

2.2 Results and Discussion

2.2.1 Selecting Quantitative Transitions

The first quadrupole of a triple quadrupole (QqQ) or quadrupole-ion trap (QIT) selects intact ions to fragment. The mass of $[M+H]^+$ for norepinephrine is 170.1, but the more stable in-source fragment is *m/z* 152.1, or $[M+H-H_2O]^+$. This means that there's normally a higher abundance of norepinephrine derived ions at *m/z* 152.1, leading to a greater abundance of fragment ions. As shown in Figure 2.2, *m/z* 107 is a unique, abundant product ion. Therefore, 152 > 107 would seem to be a judicious choice for a quantitative transition. However, while running a sample of pure epinephrine-d_6, signal was observed for the 152 > 107 transition. Since this transition state is not unique to norepinephrine, and epinephrine and norepinephrine co-elute by the chosen liquid chromatography method, it is not a viable indicator for the development of this assay.

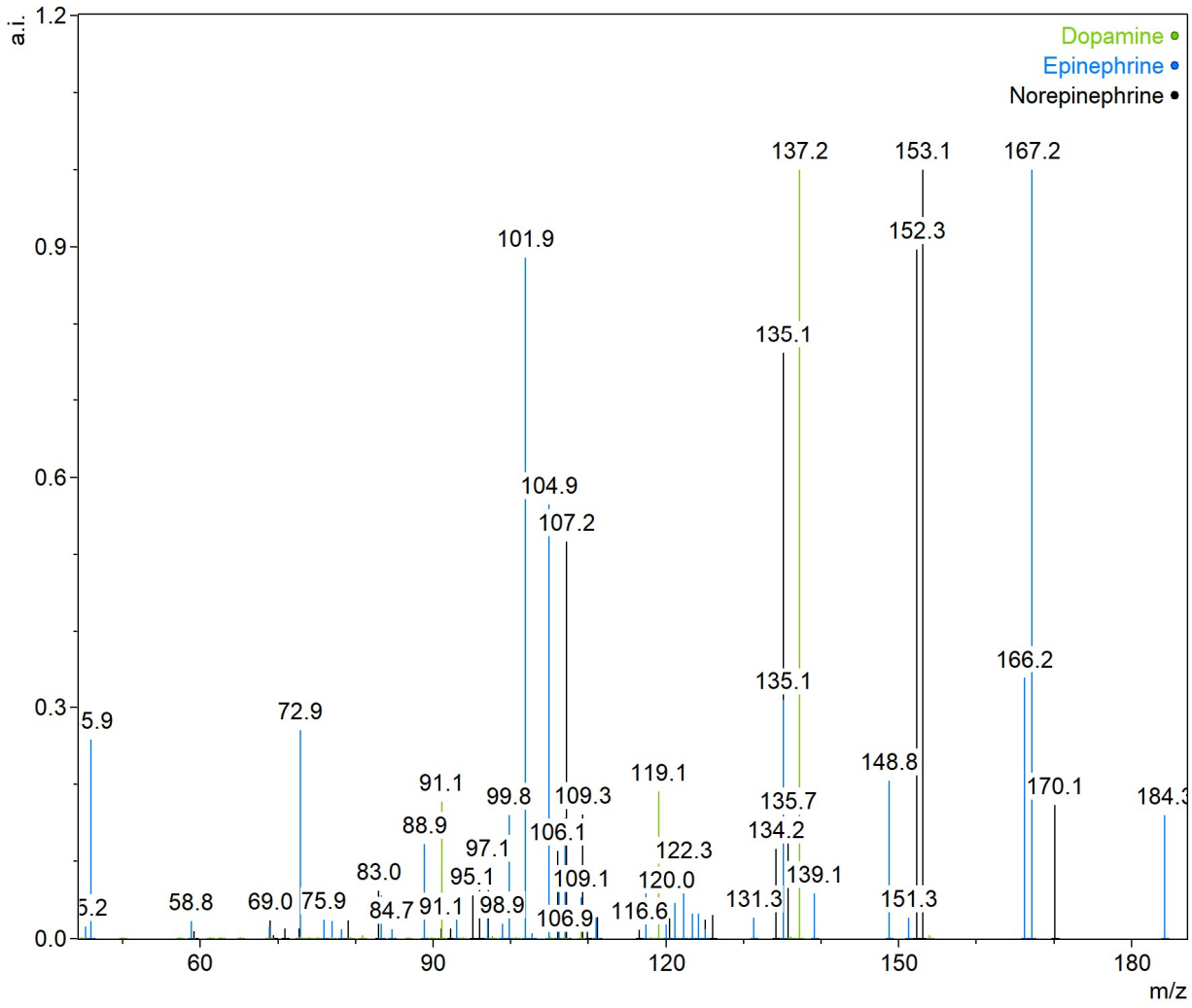

Figure 2.2. Overlaid fragmentation spectra of dopamine (green), epinephrine (blue), and norepinephrine (black). Data was sourced from MassBank[12], and the visualization was created in mMass[13].

TABLE I

MRM TRANSITION PARAMETERS

	Q1 (*m/z*)	Q3 (*m/z*)	Collision Energy (V)	Declustering Potential (V)	Entrance Potential (V)
Norepinephrine	170.1	107	22	100	9
Dopamine-d4	158.1	94	20	169	11
Epinephrine-d6	190.1	172	11	219	11

Part of selecting transitions for quantitation includes verifying linearity of the response. Transitions were first selected by examining previous literature on catecholamine assays[14,15] and further investigated by analyzing the analytes' fragmentation patterns (Figure 2.2). After selecting a transition to monitor, the mass spectrometer was tuned to determine the optimal instrument settings specific to each transition by introduction to the spectrometer direct injection. Direct injection bypasses the LC component of the system for the analysis of pure compounds. The parameters used for subsequent LC-MS/MS analysis are displayed in **Table I**.

After setting the method parameters, agarose wells consisting of equal concentration of each included catecholamine were made at 0.1 µM, 10 µM, 33 µM, 66 µM, 100 µM, 150 µM, and 200 µM. Figure 2.3 shows the calibration curve for the agarose extracts, monitored for each of the three catecholamines. Norepinephrine and dopamine-d_4 showed a consistent linear response, but epinephrine-d_6 showed a nonlinear response from 0.1-66 µM for the chosen

transition of 190.1 > 172. The r^2 value for the dopamine fit was lower, but when looking at the data the fit was mathematically less linear because of the spread of the response for each injection. However, the response associated with epinephrine was more consistent, with less variability in peak area, but follows a non-linear path, as shown in Figure 2.4.

Linearity over a wide range of concentrations was examined. We estimated that tumorigenic conditions would prompt approximately a 10 µM concentration of norepinephrine in a 300 µL well[16]. If we assumed that the concentration of epinephrine would be within the same order of magnitude as norepinephrine, then 190.1 > 172 is not a viable transition due to non-linearity.

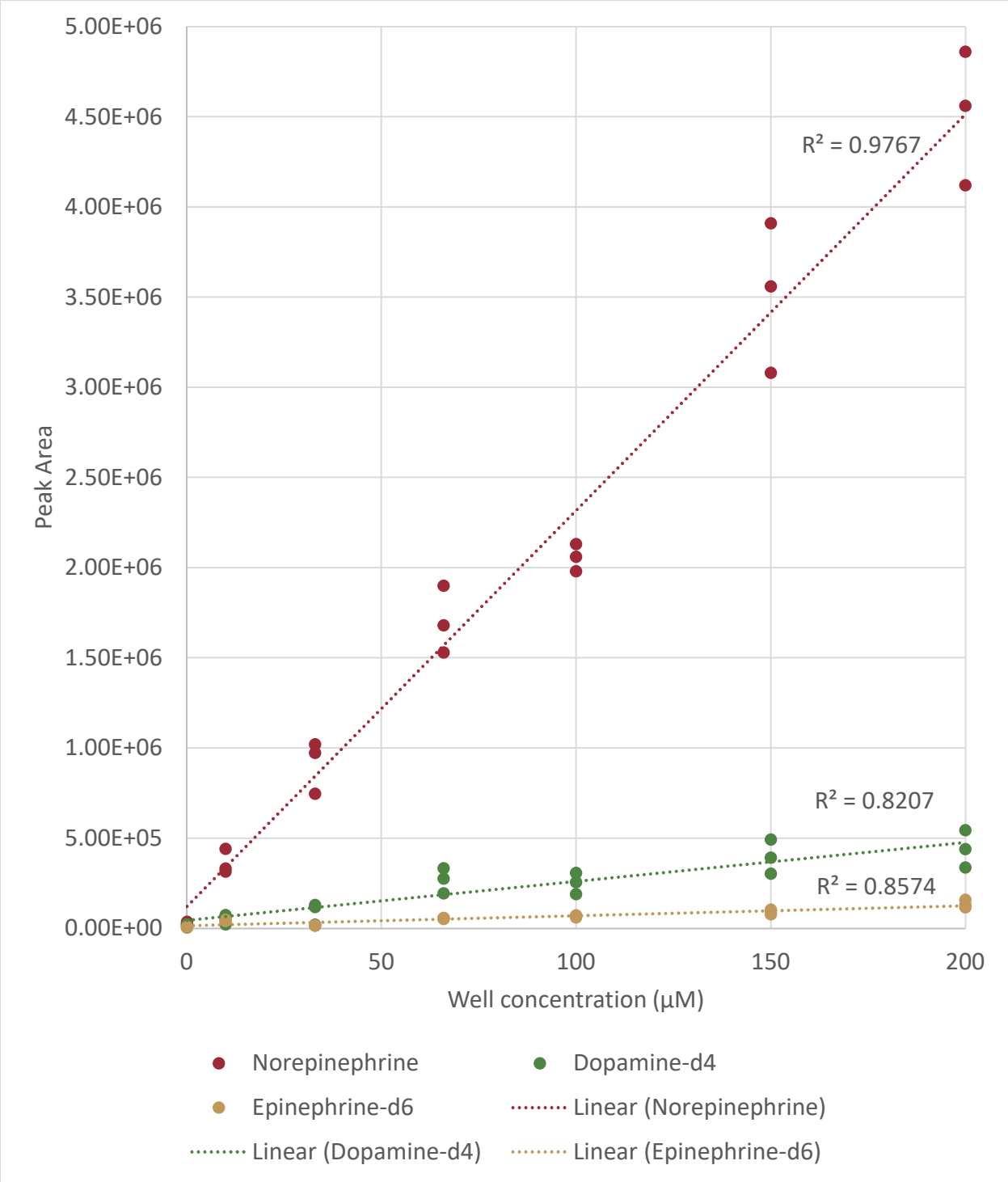

Figure 2.3 Overlay of the calibration curves relating peak area to concentration of an agarose well. Each point refers to a technical replicate for the given concentration.

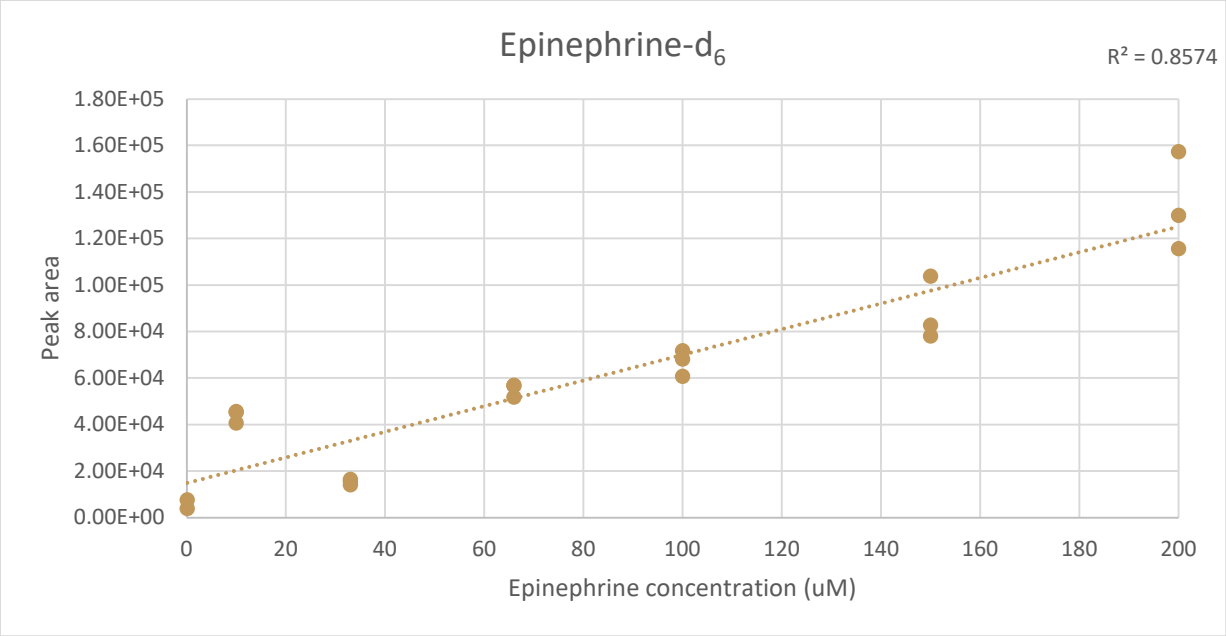

Figure 2.4. Graph of the area under the curve for the transition 190 > 172 for epinephrine stock solution with 3 technical injections each.

2.2.2 Evaluating Extraction Solvent

The catecholamines represented in this assay (**2.1-.3**) are all polar and mildly basic. The pKa for the protonated species of norepinephrine and epinephrine have been calculated to be around 8.5[17]. Thus, a selection of eight solvents were chosen to all be polar and include mildly acidic solutions. Agarose plugs were prepared by adding in pure norepinephrine bitartrate salt ($C_8H_{11}NO_3 \cdot C_4H_6O_6 \cdot H_2O$, Sigma-Aldrich) to the cell media and agarose for a final concentration of 10 mM.

TABLE II

EXTRACT INTENSITIES OBTAINED BY MALDI-TOF MS CORRESPONDING TO NOREPINEPHRINE

Solvent condition	Maximum peak height (a.u.)
Acetonitrile:Water:0.1% TFA	1150
Butanol:0.1% TFA	1030
Methanol:Water:0.1% TFA	843.0
Acetonitrile	524.0
Acetonitrile:Water	429.0
Methanol	N/A
Methanol:Water	N/A
Water	N/A

Figure 2.5 shows a comparison of all of the extraction conditions. The two extraction conditions with the highest intensity at *m/z* 170 are butanol with 0.1% trifluoroacetic acid (TFA)

and a 1:1 ratio of acetonitrile and water with 0.1% TFA. This MALDI-TOF-MS experiment is non-quantitative, so the two highest conditions were also compared by QIT-MS to achieve a higher sensitivity measurement.

The MRM experiment was set-up to monitor norepinephrine across a set of 5 calibration points, including a water blank. Figure 2.6 displays the peak areas for 170 > 107 for various agarose plug concentrations. The ACN:H_2O:TFA extraction displayed increased extraction efficiency at 100 µM and 150 µM, for increased linearity overall. Therefore, ACN:H_2O:TFA was selected as the optimal extraction solvent.

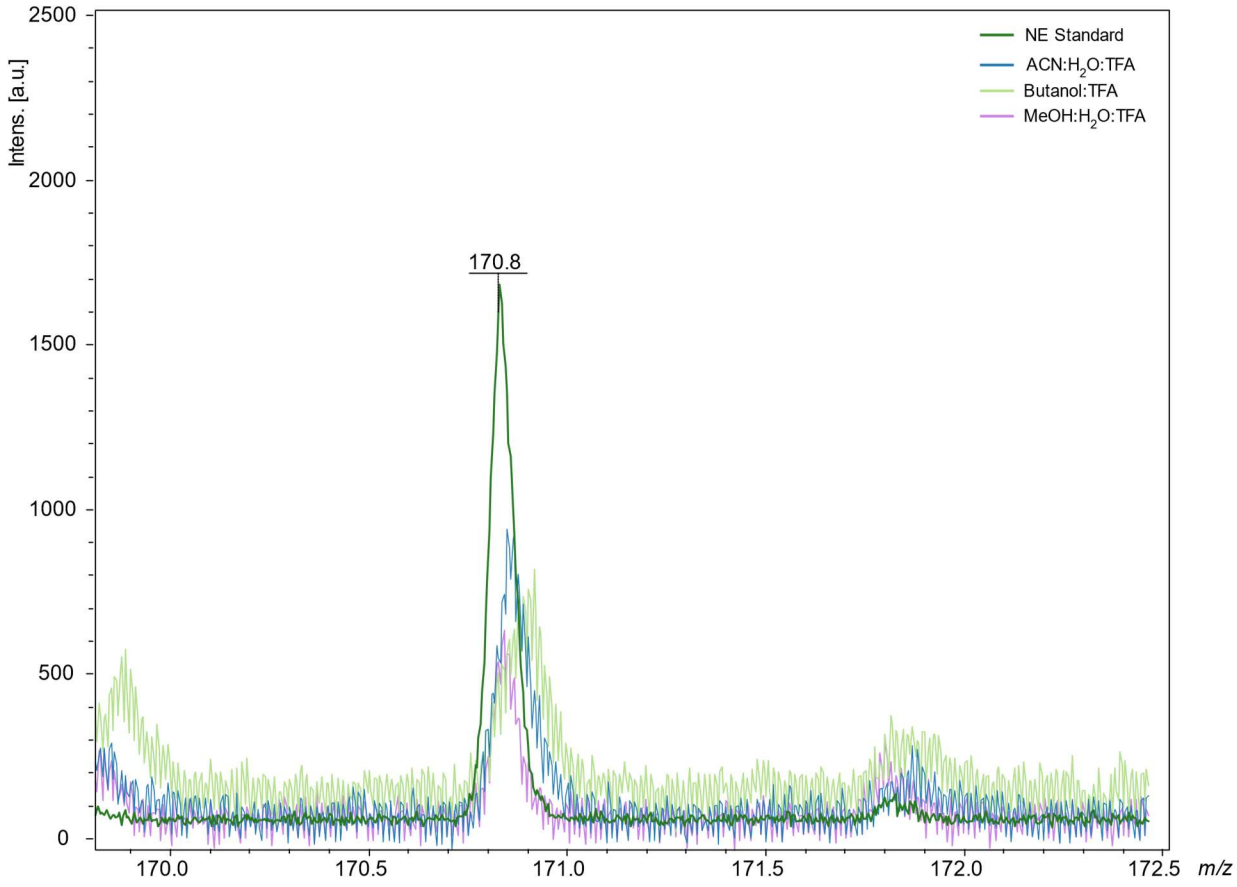

Figure 2.5. MALDI-TOF-MS spectra of agarose extractions at m/z 170, corresponding to norepinephrine.

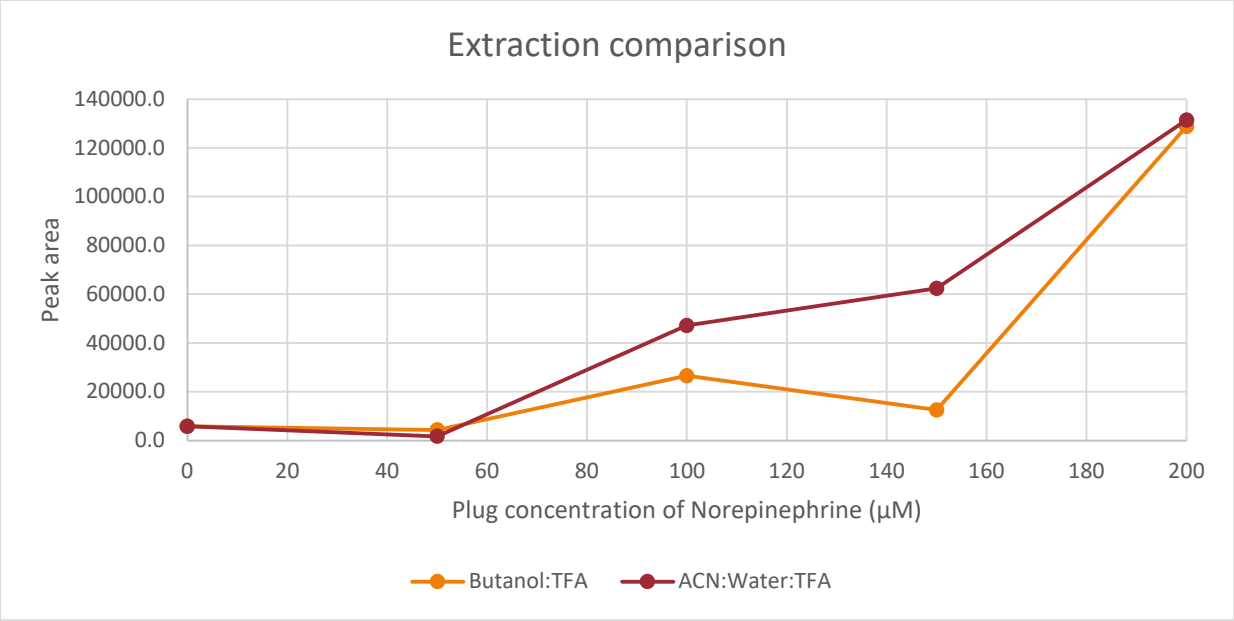

Figure 2.6. Comparison of agarose extraction solvents by MS/MS (n=1).

2.2.3 Removal of matrix by Solid Phase Extraction

After preliminary LC-MS/MS runs, the liquid chromatography column required advanced washes to reduce system pressure, indicating the column was being clogged by the agarose extracts. A SPE step, step 4 in Figure 2.1, was therefore added to reduce the need to wash the LC column during experiments.

By weight, DMEM is primarily composed of salts, D-glucose, and an assortment of amino acids[18]. The charge state of amino acids can fluctuate from -1 to +2 based on the surrounding pH and the pKa of the side chain. An appropriate sorbent for this assay would need to selectively retain analytes based on pKa. Furthermore, special attention must be made to the pH of samples prior to SPE for proper retention. The Oasis MCX sorbent is a reverse-phase cation-exchange sorbent optimized for basic compounds[19]. Proper use includes ensuring an acidic sample solution to protonate bases, performing the appropriate wash steps, followed by elution with a basic solvent[19]. A method optimized for a cell media matrix is shown in Figure 2.7.

Samples need to be acidic prior to loading onto the column so that the catecholamines will have a positively charged amine to interact with the negatively charged stationary phase. Limiting the sample preparation to an overall pH of 6 was designed to keep a majority of the amino acids in their neutral, zwitterionic state. Although the ions will have a localized positive charge, their affinity to the stationary phase should be lower than the positively charged catecholamines. Waters Corporation recommends eluting tryptic peptides in 2% ammonium hydroxide in 60:40 water:acetonitrile on MCX columns[20], which is unfortunately too similar to the catecholamine elution solvent to be used as a wash. The second wash, 60:40

methanol:acetonitrile, was designed as an alternative in this assay. Additionally, the first wash will remove polar negatively charged ions and polar neutral molecules. The final elution step is a strong base which will remove the proton from the charged catecholamines and free them from the stationary phase.

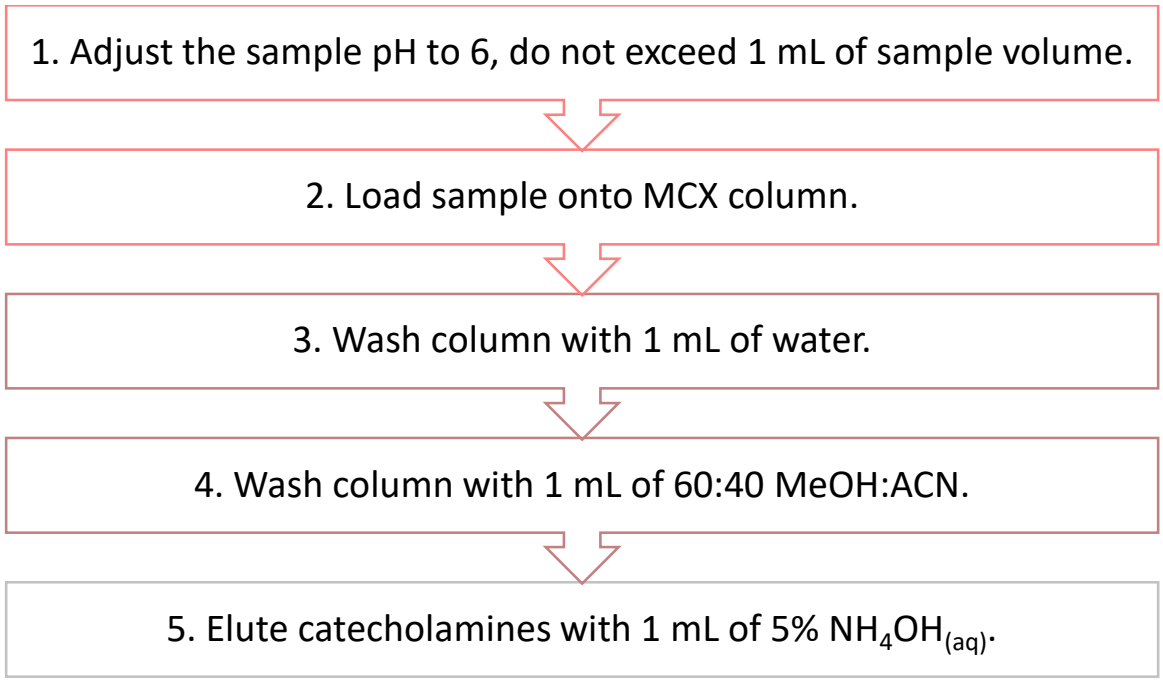

Figure 2.7. SPE method for sample cleanup.

During method development, each stage of the fractionation was collected for analysis by MALDI-TOF MS to ensure no catecholamines were lost during wash steps. Additional washes such as a basified methanolic wash and an acidified aqueous wash were excluded from the protocol based on the observation of minor amounts of catecholamines eluting with the wash. Figure 2.8 shows the MALDI-TOF-MS dried drop spectra of an initial extract overlaid with spectra of the elution fraction and a norepinephrine bitartrate stock solution.

The SPE step was introduced to clean up matrix compounds, namely amino acids and salts. Unfortunately, the mass range for many amino acids was also the range for CHCA:DHB (alpha-cyano-4-hydroxycinnamic acid: 2,5,-dihydrobenzoic acid) matrix crystals (*m/z* 100-200) so it is difficult to easily spot the presence or absence of amino acids by MALDI-TOF-MS. However, Figure 2.9 shows that there are compounds being removed in the process. The removal of sample matrix will aid in enhancing ionization of the analytes and potentially lower the limit of detection (LOD) for the assay.

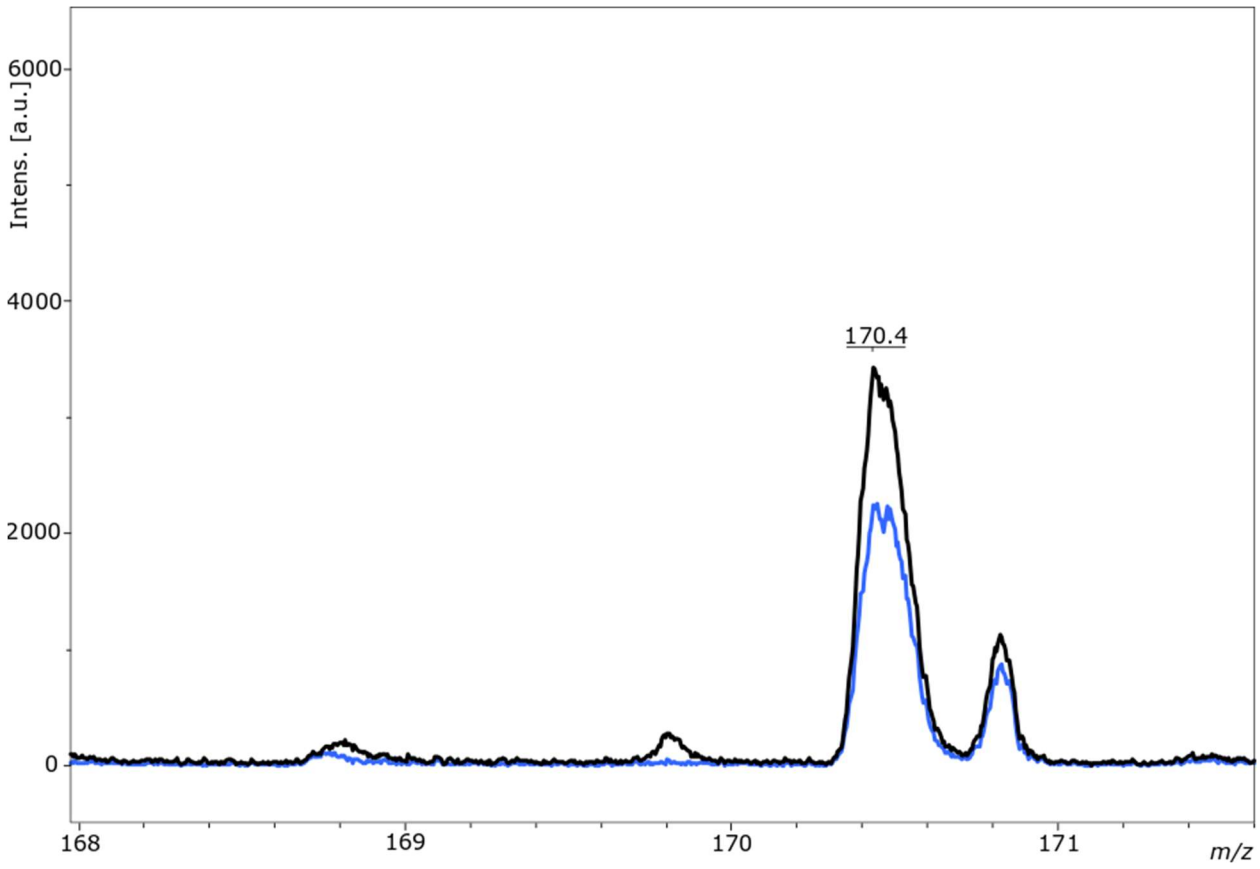

Figure 2.8. An overlay of MALDI-TOF MS spectra for the unfiltered extract (black), and the elution fraction (blue) at m/z *170.*

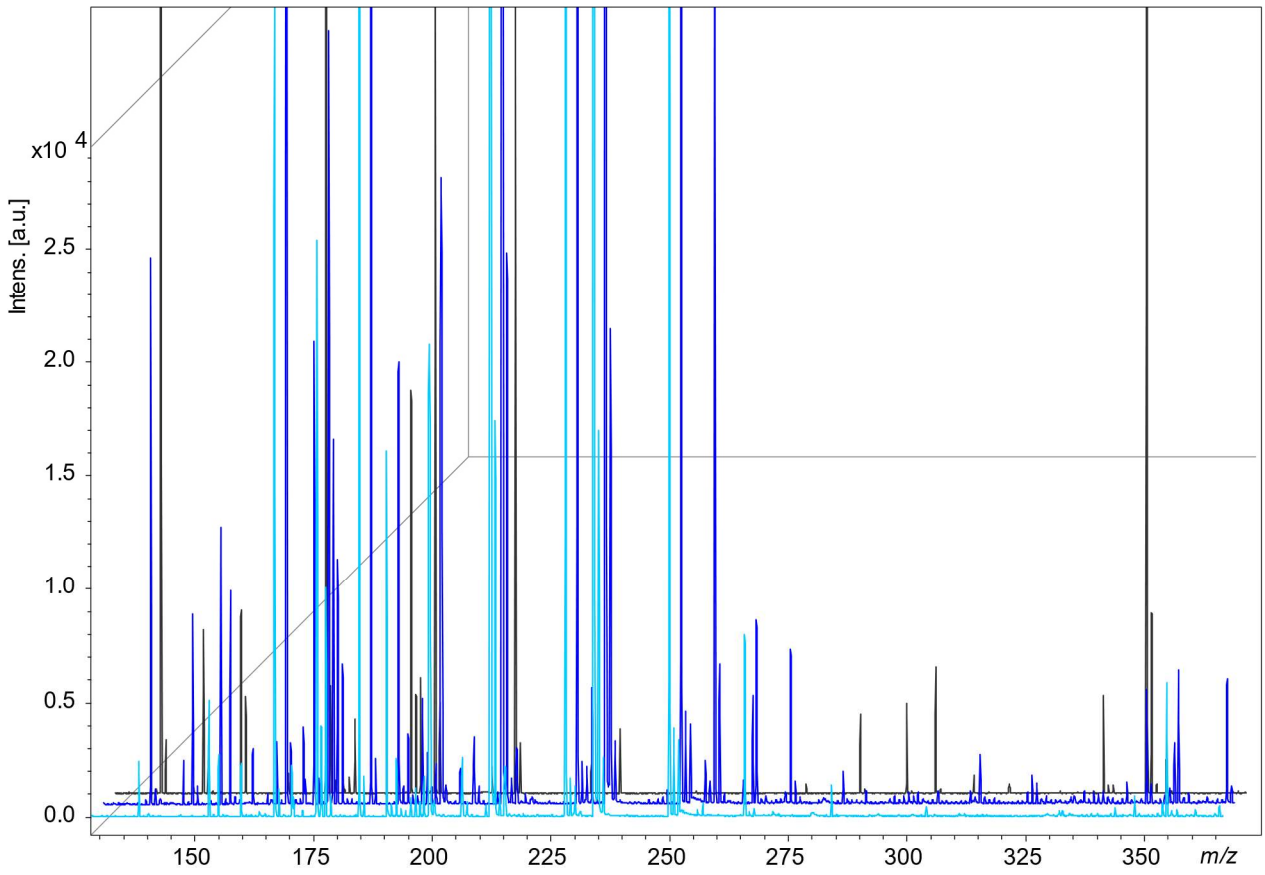

Figure 2.9. Offset overlay of a MALDI-TOF-MS sum spectrum of the original extract (dark blue), elute fraction (light blue), and matrix blank from m/z 150 to m/z 350.

2.3 Conclusion

Extraction and purification of catecholamines from DMEM agarose has been well optimized for the purpose of this assay. However, additional work is necessary to select the idealMS/MS transitions. Overall, the MRM transition parameters need to be optimized by following researchers during the development of new assays or if using a different instrument, but the sample preparation methods outlined are viable for all catecholamine extractions from DMEM agarose. Additionally, previous literature[10,21] only describes sample extraction from liquid cell culture, making this the first report of extraction from a solid cell media matrix.

2.4 Experimental

2.4.1 Agarose plugs

Low melting agarose plugs were made following the protocols stated in the original manuscript[5], but the ITO-coated slide was substituted with a plastic slide and 8-well chamber. To prepare each well, 200 μL of 2X DMEM was mixed with 200 μL of 2% low melting agarose liquified at 70°C for a final concentration of 1X DMEM per well. 300 μL of the mixture was aliquoted per well. If the wells needed to have a concentration of norepinephrine, 6.78 μL of aqueous norepinephrine bitartrate salt solutionwas added to the aforementioned 400 μL of cell media and agarose before aliquotting 300 μL into the chambered slide. The concentration of the norepinephrine solution was prepared to be 60 times more concentrated than the desired well concentration.The slide was left to incubate overnight at 5% CO_2 and 37 °C to mimic any degredation that would occur during studies with cells.

2.4.2 Extraction

Low melting agarose plugs containing norepinephrine standard were individually placed into 1.8 mL microcentrifuge tubes and frozen at -70 C. Samples were thoroughly lyophilized, and then macerated with a fresh toothpick. 1 mL of 50:50 acetonitrile:water with 0.1% TFA was added to each sample and the extractions were sonicated for 1 h. The extractions were then centrifuged at 10k rpm for 2 min. The supernatant was transferred to a new vial before adding 150 µL of acetonitrile to dehydrate any agarose that was rehydrated during the extraction process and to ensure all supernatant was transferred. Resulting extracts were dried *in vacuo*.

2.4.3 MALDI-TOF Dry Drop Analysis

MS data was collected in positive reflection mode on an Autoflex Speed LRF mass spectrometer (Bruker Daltonics) over the mass range 100-1000 Da. The smartbeam-II laser (355 nm) was operated at size 3, medium, and 4,000 shots. Laser power was set between 40-60% with a gain of 9.0x. Extracts were spotted on a ground steel 96 target plate in a 1:1 ratio with recrystallized 1:1 CHCA:DHB matrix. The instrument was calibrated manually using phosphorus red. Signals below *m/z* 80 were suppressed.

2.4.4. Parameter Optimization

Optimization of the collision energy, declustering potential, and entrance potential for standards in **Table I** was accomplished through direct infusion of single analytes at 10 ng/mL on a SCIEX Triple Quad™ 5500. The syringe pump was set to a flow rate of 10 µL/min. Each parameter was optimized using the ramping feature of the instrument and selecting the voltage that produced the highest intensity over the course of 5 technical replicates.

2.4.4 MRM Analysis

The MRM assay was performed on a SCIEX Triple Quad™ 5500+ LC-MS/MS System interfaced with an Agilent 1200 Infinity series HPLC. Dried extracts were resuspended in 25 uL of Milli-Q purified water (Millipore Sigma) before injection. The chromatography gradient started at 97% A and increased to 99% A after 3 minutes, where solvent A was water purified by a Milli-Q purification system with 0.1% formic acid buffer, and solvent B was LCMS grade acetonitrile with 0.1% formic acid buffer. A 5 μL injection volume was used and a flow rate of 0.45 mL/min. A Kinetex Biphenyl 2.1x50 mm column (Phenomenex) was used for liquid chromatography. Data was processed in Skyline version 20.1.0.31[22,23] and graphed in Microsoft Excel. No weighting methods were used for determining the least square error linear regression.

2.5 Cited Literature

(1) Siegel, R. L.; Miller, K. D.; Jemal, A. Cancer Statistics, 2018. CA. Cancer J. Clin. 2018, 68 (1), 7–30. https://doi.org/10.3322/caac.21442.

(2) Ovarian Cancer - Cancer Stat Facts https://seer.cancer.gov/statfacts/html/ovary.html (accessed Mar 3, 2020).

(3) Vaughan, S.; Coward, J. I.; Bast, R. C.; Berchuck, A.; Berek, J. S.; Brenton, J. D.; Coukos, G.; Crum, C. C.; Drapkin, R.; Etemadmoghadam, D.; Friedlander, M.; Gabra, H.; Kaye, S. B.; Lord, C. J.; Lengyel, E.; Levine, D. A.; McNeish, I. A.; Menon, U.; Mills, G. B.; Nephew, K. P.; Oza, A. M.; Sood, A. K.; Stronach, E. A.; Walczak, H.; Bowtell, D. D.; Balkwill, F. R. Rethinking Ovarian Cancer: Recommendations for Improving Outcomes. Nat. Rev. Cancer 2011, 11 (10), 719–725. https://doi.org/10.1038/nrc3144.

(4) Bowtell, D. D.; Böhm, S.; Ahmed, A. A.; Aspuria, P.-J.; Bast, R. C.; Beral, V.; Berek, J. S.; Birrer, M. J.; Blagden, S.; Bookman, M. A.; Brenton, J. D.; Chiappinelli, K. B.; Martins, F. C.; Coukos, G.; Drapkin, R.; Edmondson, R.; Fotopoulou, C.; Gabra, H.; Galon, J.; Gourley, C.; Heong, V.; Huntsman, D. G.; Iwanicki, M.; Karlan, B. Y.; Kaye, A.; Lengyel, E.; Levine, D. A.; Lu, K. H.; McNeish, I. A.; Menon, U.; Narod, S. A.; Nelson, B. H.; Nephew, K. P.; Pharoah, P.; Powell, D. J.; Ramos, P.; Romero, I. L.; Scott, C. L.; Sood, A. K.; Stronach, E. A.; Balkwill, F. R. Rethinking Ovarian Cancer II: Reducing Mortality from High-Grade Serous Ovarian Cancer. Nat. Rev. Cancer 2015, 15 (11), 668–679. https://doi.org/10.1038/nrc4019.

(5) Zink, K. E.; Dean, M.; Burdette, J. E.; Sanchez, L. M. Imaging Mass Spectrometry Reveals Crosstalk between the Fallopian Tube and the Ovary That Drives Primary Metastasis of Ovarian Cancer. ACS Cent. Sci. 2018, 4 (10), 1360–1370. https://doi.org/10.1021/acscentsci.8b00405.

(6) Lamouroux, A.; Vigny, A.; Faucon Biguet, N.; Darmon, M. C.; Franck, R.; Henry, J. P.; Mallet, J. The Primary Structure of Human Dopamine-Beta-Hydroxylase: Insights into the Relationship between the Soluble and the Membrane-Bound Forms of the Enzyme. EMBO J. 1987, 6 (13), 3931–3937.

(7) Kanehisa, M. KEGG: Kyoto Encyclopedia of Genes and Genomes. Nucleic Acids Res. 2000, 28 (1), 27–30. https://doi.org/10.1093/nar/28.1.27.

(8) Kanehisa, M. Toward Understanding the Origin and Evolution of Cellular Organisms. Protein Sci. 2019, 28 (11), 1947–1951. https://doi.org/10.1002/pro.3715.

(9) Kanehisa, M.; Sato, Y.; Furumichi, M.; Morishima, K.; Tanabe, M. New Approach for Understanding Genome Variations in KEGG. Nucleic Acids Res. 2019, 47 (D1), D590–D595. https://doi.org/10.1093/nar/gky962.

(10) Halama, A. Metabolomics in Cell Culture—A Strategy to Study Crucial Metabolic Pathways in Cancer Development and the Response to Treatment. Arch. Biochem. Biophys. 2014, 564, 100–109. https://doi.org/10.1016/j.abb.2014.09.002.

(11) Duncan, M.; Gale, P.; Yergey, A. The Principles of Quantitative Mass Spectrometry, 1st ed.; Rockpool Productions: Colorado, 2006.

(12) Horai, H.; Arita, M.; Kanaya, S.; Nihei, Y.; Ikeda, T.; Suwa, K.; Ojima, Y.; Tanaka, K.; Tanaka, S.; Aoshima, K.; Oda, Y.; Kakazu, Y.; Kusano, M.; Tohge, T.; Matsuda, F.; Sawada, Y.; Hirai, M. Y.; Nakanishi, H.; Ikeda, K.; Akimoto, N.; Maoka, T.; Takahashi, H.; Ara, T.; Sakurai, N.; Suzuki, H.; Shibata, D.; Neumann, S.; Iida, T.; Tanaka, K.; Funatsu, K.; Matsuura, F.; Soga, T.; Taguchi, R.; Saito, K.; Nishioka, T. MassBank: A Public Repository for Sharing Mass Spectral Data for Life Sciences. J. Mass Spectrom. 2010, 45 (7), 703–714. https://doi.org/10.1002/jms.1777.

(13) Strohalm, M.; Kavan, D.; Novák, P.; Volný, M.; Havlíček, V. MMass 3: A Cross-Platform Software Environment for Precise Analysis of Mass Spectrometric Data. Anal. Chem. 2010, 82 (11), 4648–4651. https://doi.org/10.1021/ac100818g.

(14) Zhu, K. Y.; Fu, Q.; Leung, K. W.; Wong, Z. C. F.; Choi, R. C. Y.; Tsim, K. W. K. The Establishment of a Sensitive Method in Determining Different Neurotransmitters Simultaneously in Rat Brains by Using Liquid Chromatography–Electrospray Tandem Mass Spectrometry. J. Chromatogr. B 2011, 879 (11–12), 737–742. https://doi.org/10.1016/j.jchromb.2011.02.011.

(15) Whiting, M. J. Simultaneous Measurement of Urinary Metanephrines and Catecholamines by Liquid Chromatography with Tandem Mass Spectrometric Detection. Ann. Clin. Biochem. 2009, 46 (2), 129–136. https://doi.org/10.1258/acb.2008.008180.

(16) Sood, A. K.; Bhatty, R.; Kamat, A. A.; Landen, C. N.; Han, L.; Thaker, P. H.; Li, Y.; Gershenson, D. M.; Lutgendorf, S.; Cole, S. W. Stress Hormone-Mediated Invasion of Ovarian Cancer Cells. Clin. Cancer Res. Off. J. Am. Assoc. Cancer Res. 2006, 12 (2), 369–375. https://doi.org/10.1158/1078-0432.CCR-05-1698.

(17) Álvarez-Diduk, R.; Galano, A. Adrenaline and Noradrenaline: Protectors against Oxidative Stress or Molecular Targets? J Phys Chem B 2015, 119 (8), 3479–3491. https://doi.org/10.1021/acs.jpcb.5b00052.

(18) HiMedia Laboratories Pvt. Ltd. Dulbecco's Modified Eagle Medium (DMEM). HiMedia Laboratories Pvt. Ltd.

(19) Waters Corporation. Oasis Care and Use Manual. Waters Corporation December 2017.

(20) Waters Corporation. ProteinWorks Microelution SPE Clean-Up Kit. Waters Corporation January 2016.

(21) Čuperlović-Culf, M.; Barnett, D. A.; Culf, A. S.; Chute, I. Cell Culture Metabolomics: Applications and Future Directions. Drug Discov. Today 2010, 15 (15–16), 610–621. https://doi.org/10.1016/j.drudis.2010.06.012.

(22) Adams, K. J.; Pratt, B.; Bose, N.; Dubois, L. G.; St.John-Williams, L.; Perrott, K. M.; Ky, K.; Kapahi, P.; Sharma, V.; MacCoss, M. J.; Moseley, M. A.; Colton, C. A.; MacLean, B. X.; Schilling, B.; Thompson, J. W. Skyline for Small Molecules: A Unifying Software Package for Quantitative Metabolomics. J. Proteome Res. 2020, acs.jproteome.9b00640. https://doi.org/10.1021/acs.jproteome.9b00640.

(23) Pino, L. K.; Searle, B. C.; Bollinger, J. G.; Nunn, B.; MacLean, B.; MacCoss, M. J. The Skyline Ecosystem: Informatics for Quantitative Mass Spectrometry Proteomics. Mass Spectrom Rev 2017.

2.6 Bibliography

Bicker, J.; Fortuna, A.; Alves, G.; Falcão, A. Liquid Chromatographic Methods for the Quantification of Catecholamines and Their Metabolites in Several Biological Samples–a Review. *Anal. Chim. Acta* **2013**, *768*, 12–34.

CHAPTER 3. DEVELOPMENT OF A UNIQUE MICROBIAL LIBRARY SAMPLED FROM *HETEROCEPHALUS GLABER* TISSUE

3.1 Introduction

Naked mole rats (*Heterocephalus glaber*) have been widely researched for their long lifespan[1,2], ability to survive hypoxic environments[3,4], intolerance to pain[5], and resistance to cancer[6,7]. *In vitro* study of mammalian cells , our collaborators and their colleagues have had difficulty with unusual microbial "contaminants" while attempting to culture skin fibroblasts from *H. glaber*. Due to repeated observations of this phenomenon, we hypothesized that the so-called "contaminants" may be commensal microbes.

Screening libraries are collections of chemicals, either pure or as a mixture, used in conjunction with disease specific bioassays to screen for drug leads. Libraries can be comprised of synthetic chemicals as well as natural product extracts or purified compounds. Concerns have arisen regarding the large amount of biomass needed to fully identify an active molecule from natural sources[8]. Researchers are increasingly turning to microbes as powerful, renewable cellular machines for producing bioactive metabolites[8–10]. Figure 3.1 shows a microbial library generation process as applied to this project.

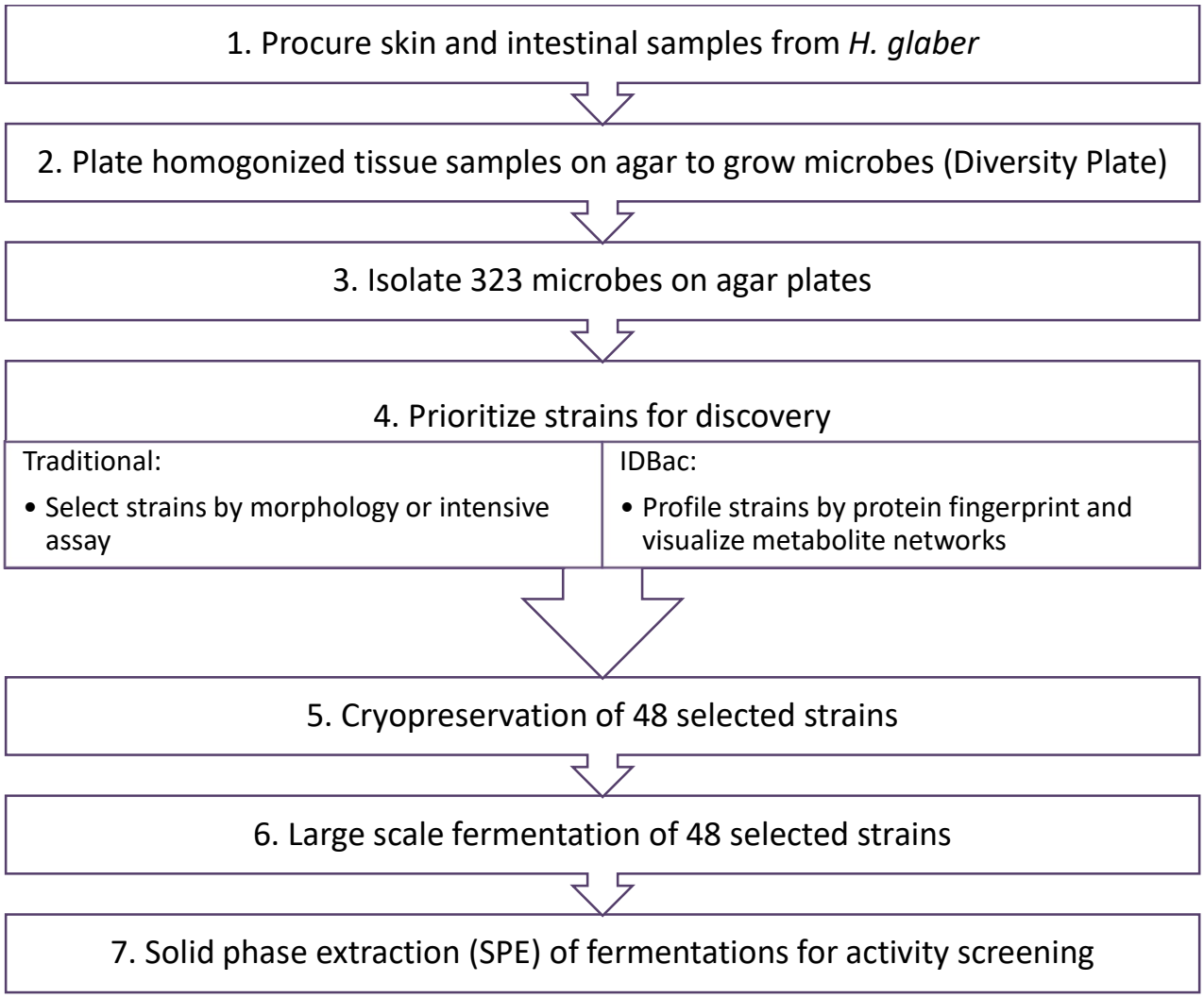

Figure 3.1. Project overview. Steps 6 and 7 are future directions for the project.

A microbial presence in the skin drove the hypothesis for the project but it was decided to also source the intestinal tissue. Mammalian microbiomes have been proven to be viable sources of bioactive molecules[11–16], and naked mole rats have been shown to have a unique gut microbiome compared to other mammals[17]. The gut has also been linked to overall human health[18–20], and the same may be true in *H. glaber*. Even if there is no correlation between the health of *H. glaber* and its microbial partners, the novelty of the *H. glaber* as a niche environment may still lead to unique molecules from a discovery pipeline.

3.1.1 Media Selection can Impact Microbial Diversity in Library Selection

The first step in library generation is the "diversity" plate. A diversity plate provides a broad span of microbes the nutrient combinations they need to propagate in the laboratory setting. The level and type of nutrients (i.e. simple carbon and nitrogen vs complex carbon and nitrogen), or the addition of antibiotics or antifungals determines what microbes may propagate on the plate. If the media is too nutrient rich, the plate may become quickly overgrown with common microbes. Likewise, if the media lacks nutrients, it may be too hostile to foster growth.

Fungal growth media tends to be rich in carbohydrates, which acts as a source of carbon for cellular synthesis[21]. Different species of fungi can utilize simple carbon sources such as glucose or amino acids, while others can use more complex sources like keratin and lignin. The majority of filamentous fungi utilize carbohydrates like monosaccharides, starch, and cellulose[21]. One media condition, simple nutrient fiber plus fiber (SNF + Fiber)[22], was designed to mimic a gut environment by utilizing insoluble fiber. The media had previously been shown to be able to cultivate gut-derived bacteria, and we hypothesize that the fiber could be an

ample carbon source for fungi as well[22]. SNF + Fiber otherwise lacks any other nutrients. Gause Modified Freshwater (GMF)[23] was used as a slightly more nutrient rich medium. In addition, to curb the growth of fast-growing microbes and select for both fungi and bacteria, half of the plates had an anti-fungal agent added while the other half had an antibiotic added.

3.1.2 Protein and Metabolite Profiling (IDBac) with MALDI-TOF MS

After colonies become visible on the diversity plates, they are transferred to individual isolate plates to ensure the purity of the colony. Once the colony has been determined to be pure, the microorganism is profiled by MALDI-TOF MS using the open source platform IDBac[24], introduced in section 1.4. Microorganisms form groups based on their protein similarities. Then, users can view the MALDI-TOF-MS metabolite association network (MAN) of any given number of strains to identify unique metabolite production based on features. This process allows for selecting a library that is both taxonomically diverse and varied in metabolite production potential.

3.1.3 Isolate Name Code

The name of each isolate is based on the conditions under which it was isolated. The letters before each isolate ID number stand for the tissue source and media condition. K1 stands for the first skin sample, K2 stands for the second skin sample, M stands for the small intestine and L represents the large intestine. A following G denotes GMF media, while a following F denotes SNF media. Bacteria are numbered by their pseudophylogeny group followed by their identifier within the group. There is no group marker for fungi, only an isolate number. There is no overlap in fungi isolate numbers e.g. only one isolate ends in -001.

3.2 Results and Discussion

Across all of the diversity plates, 323microbial isolates grew and were profiled. The ultimate goal of the library will be to generate a 384-well plate of fractionated extracts.. This project was designed to be a small experimental library, so one 384-well plate functions as a complete unit for high throughput screening. Since the chosen fractionation scheme results in seven fractions per extract[25], there will be room for approximately 48 isolates in the library.Since the project first began as an investigation of a fungi, itwas decided to favor isolated fungi within the library for a goal of selecting24 bacteria and 24 fungi for preservation in cryostorage and subsequent fermentation and fractionation

3.2.1 Fungal Library Prioritization

Of 323 isolates profiled, 50 were identified as fungi based on morphology. Yeast tend to be off-white and mucosal, similar to bacteria, and so it is possible some yeast species may be identified as bacteria based on morphology. However, yeasts are used as biosynthetic hosts for natural product synthesis precisely because they are known for a lack of unique secondary metabolite production[26]. It is unlikely that a yeast's metabolic diversity would surpass any bacterium it may be grouped with during the profiling steps. Figure 3.2 shows the dendrogram generated from the fungal protein fingerprint along with seed strains with known identities provided by a collaborator lab.

Upon seeding the pseudodendrogram, two major clades arose. The first clade, marked with green lines within the pseudodendrogram in Figure 3.2, seeded with two cheese rind-derived *Penicillium* strains indicating a possible genus identity for other isolates within the clade. It is worth noting that *Penicillium camemberti* did not clade with the other *Penicillium*

species. Mass spectrometry methods for taxonomic identification of microbes is not fully capable of charting higher order phylogeny, and this can sometimes apply even at the genus level[27].

Near the bottom of the pseudodendrogram, *Debaryomyces sp.* claded with three isolates. *Debaryomyces* is a yeast, suggesting the possibility that the three isolates may also be yeasts rather than filamentous fungi. The isolates within the green, *Penicillium*-seeded clade were incorporated with the four isolates at the bottom of the pseudodendrogram to form "group A", and the large clade with no seeded fungi that shares a branch point with group A was designated "group B".

The MAN for each group was viewed separately with the goal of identifying 24 fungi to prioritize for preservation in a drug discovery library. Group B, shown in Figure 3.3, displays numerous isolates with unique nodes. The highlighted isolates from Figure 3.3 and Figure A.12 were first used to inoculate 90 mm ISP-2 agar plates to generate a large quantity of spores for preservation. However, upon also inoculating ISP-2 agar plates made with 25 mg/L of cycloheximide, resulting bacterial growth indicated that 75% of the chosen isolates listed in **Table III** were a visually homogenous culture of both bacteria and fungi. It was hypothesized that the selected isolates displayed so many unique nodes precisely because a mixture of bacterial and fungal metabolites were being represented at each "single isolate". It was determined that efforts would be made to isolate strictly the chosen fungal strains, and run another dry drop extraction before finalizing the decision to migrate the strains to cryopreservation.

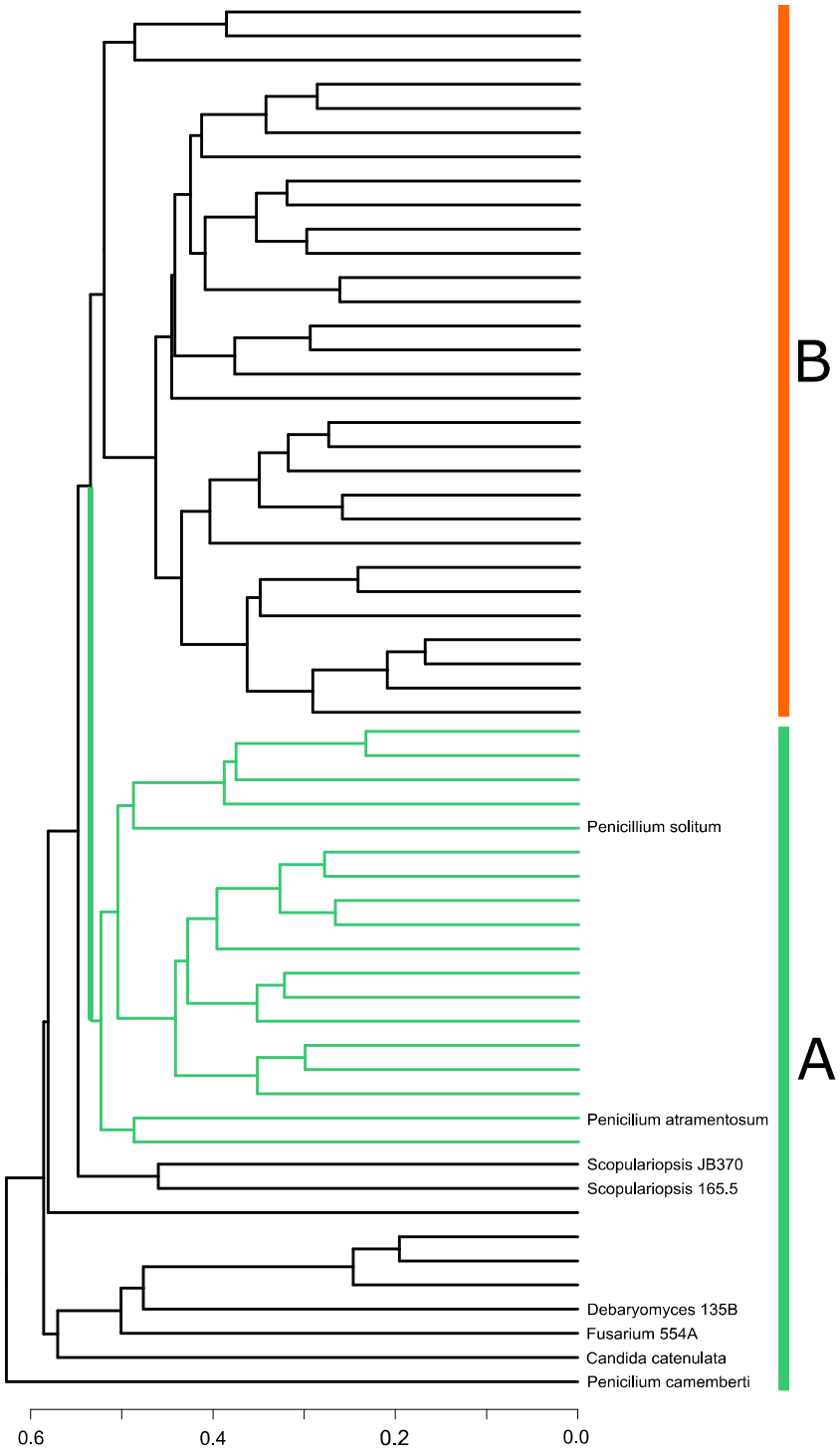

Figure 3.2. Pseudophylogenetic dendrogram created from MALDI-TOF MS protein profiling of isolated fungi seeded with identified fungal strains. Identified strains are denoted by their taxonomic name or identifier.

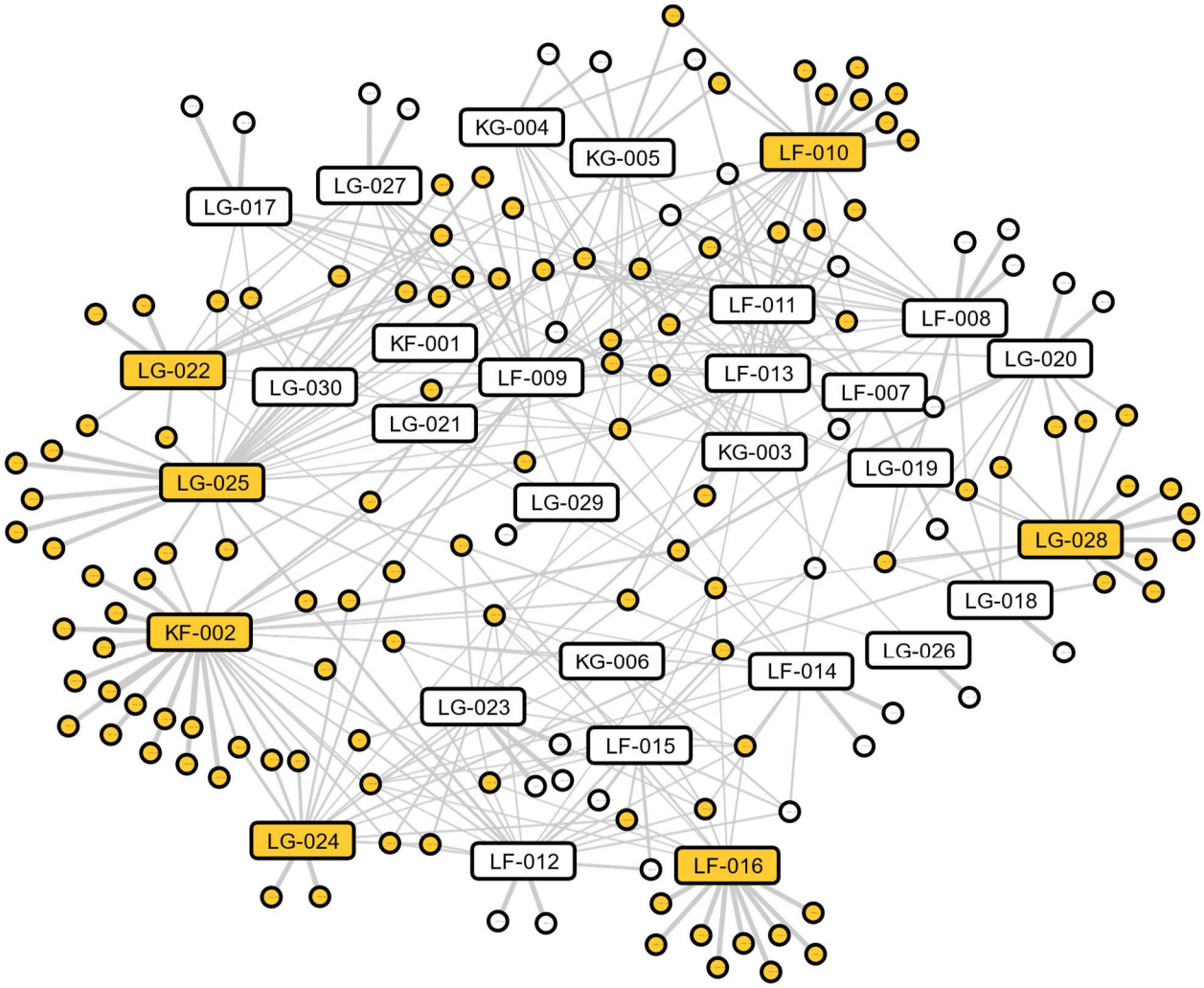

Figure 3.3. Metabolite association network of fungal isolates in clade B. Library isolates and their connected metabolite nodes are in orange.

TABLE III

Library Fungi Metadata

Group	Isolate name	Tissue source	Media type	Plating method	First inoculated on
A	LF-030	Lg. intestine	SNF	Undiluted spread	7/1/2019
	LG-031	Lg. intestine	GMF	Undiluted spread	7/2/2019
	LG-032	Lg. intestine	GMF	Undiluted spread	7/2/2019
	LF-033	Lg. intestine	SNF	Undiluted spread	7/2/2019
	LF-034	Lg. intestine	SNF	Undiluted spread	6/29/2019
	LG-035	Lg. intestine	GMF	Undiluted spread	7/2/2019
B	LF-010	Lg. intestine	SNF	Undiluted spread	6/29/2019
	LG-022	Lg. intestine	GMF	Undiluted spread	7/2/2019
	LG-025	Lg. intestine	GMF	Undiluted spread	7/2/2019
	LF-016	Lg. intestine	SNF	1:100 spread	09/27/2019
	LG-024	Lg. intestine	GMF	Undiluted spread	7/2/2019
	K1F-002	Skin	SNF	1:100 spread	7/2/2019
	LG-028	Lg. intestine	GMF	Undiluted spread	7/2/2019

3.2.2 Bacteria Library Prioritization

The authors of IDBac have suggested reviewing large sets of microbes by making groupings based on pseudophylogeny[28]. At the outset of the project it was decided to generate a library with 24 bacterial isolates, therefore based on Costa et al., the aim would be to divide the pseudodendrogram into 12 groups and to select two isolates from each group[28]. One option would be to cut the pseudodendrogram at a given modularity score, however Figure 3.4 shows how the generated dendrogram has a sloped quality. Cutting the pseudodendrogram at, for example, 0.6 would generate nine groups each consisting of only a few isolates, along with an overwhelming group of over 200 isolates. Instead, it was decided to first evenly divide the pseudodendrogram into 12 even groupings of 22-23 isolates each. After the even cut, boundaries between groups were adjusted to maximize the pseudodendrogram height that determined the division. Essentially, groupings were adjusted through localized height cutting to avoid separating closely related isolates. Figure 3.4 displays the final groups.

The MAN of each group was used to then select which isolates would be preserved based on the total number of connecting metabolite nodes and the number of metabolite nodes unique to only that isolate. Additionally, after selecting two candidates, the amount of overlap between the two isolates was considered. The two isolates should together cover as many nodes of the MAN as possible. An example of one such network and the selected isolates can be found in

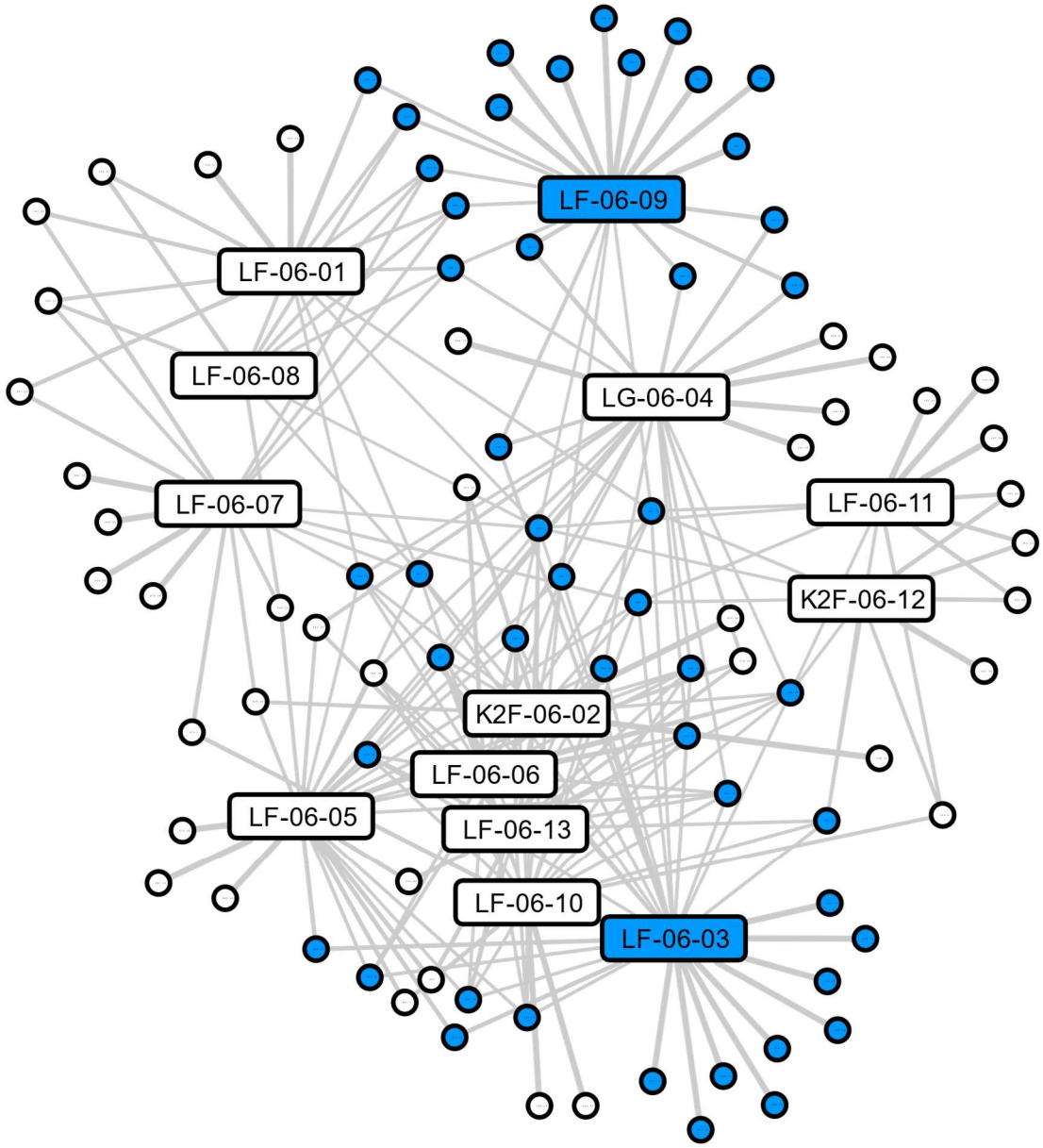

Figure 3.5. LF-06-03 has 30 associated ions, and 9 of them are unique. LF-06-09 also has 9 unique ions, and 22 associated ions total. LF-06-05 in comparison has 28 associated ions, however it was not selected for the library. Despite having more associated ions than LF-06-09, it shares many of its nodes with LF-06-03, and only has 3 unique ions. Therefore, because LF-06-09 would add more overall coverage of the network, including a large number of unique ions, it

was ultimately chosen over LF-06-05. ***Table IV*** *lists all of the chosen strains across bacteria groups 1-12.*

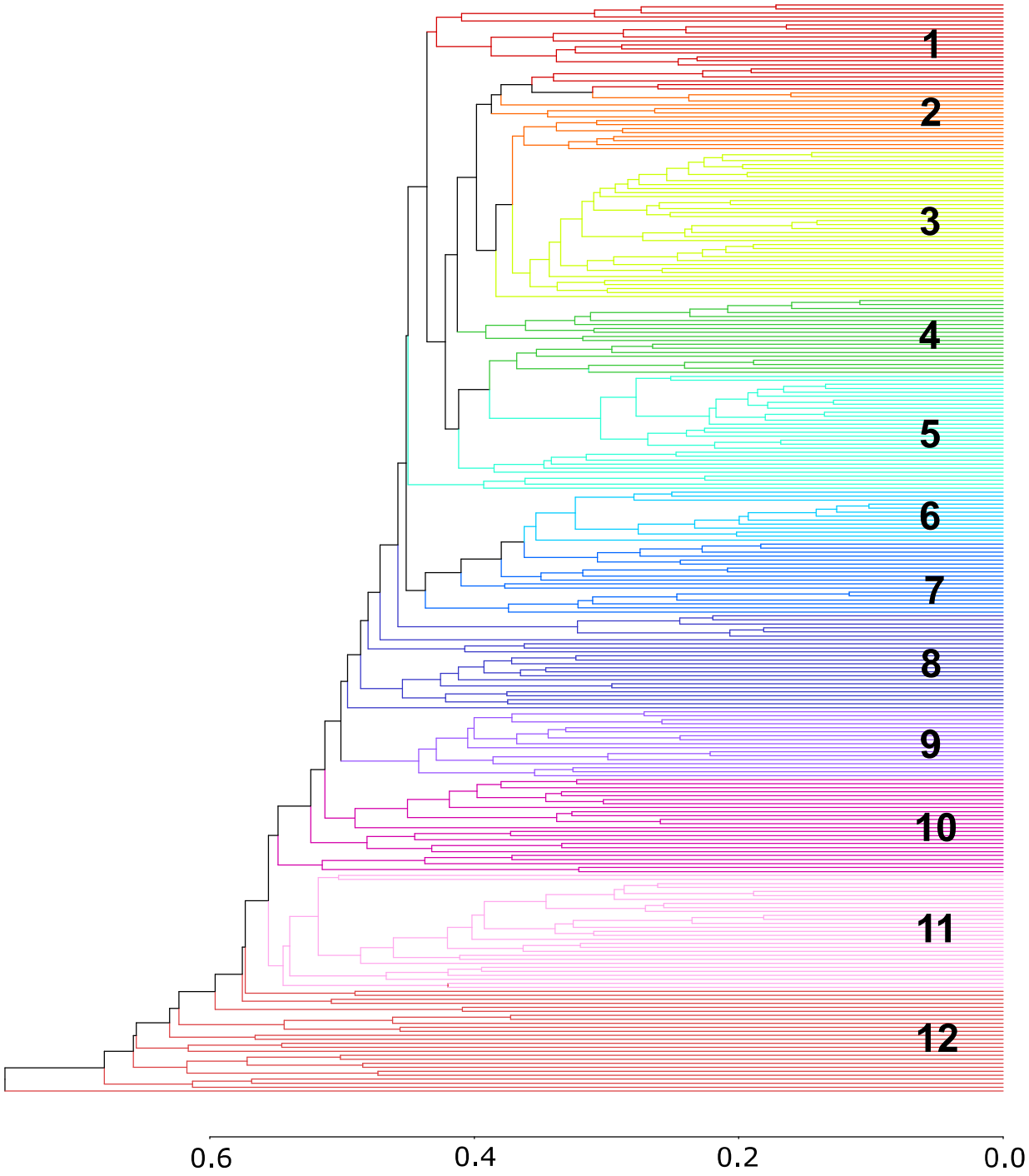

Figure 3.4. Pseudophylogenetic dendrogram created from MALDI-TOF MS protein profiling of bacteria isolates

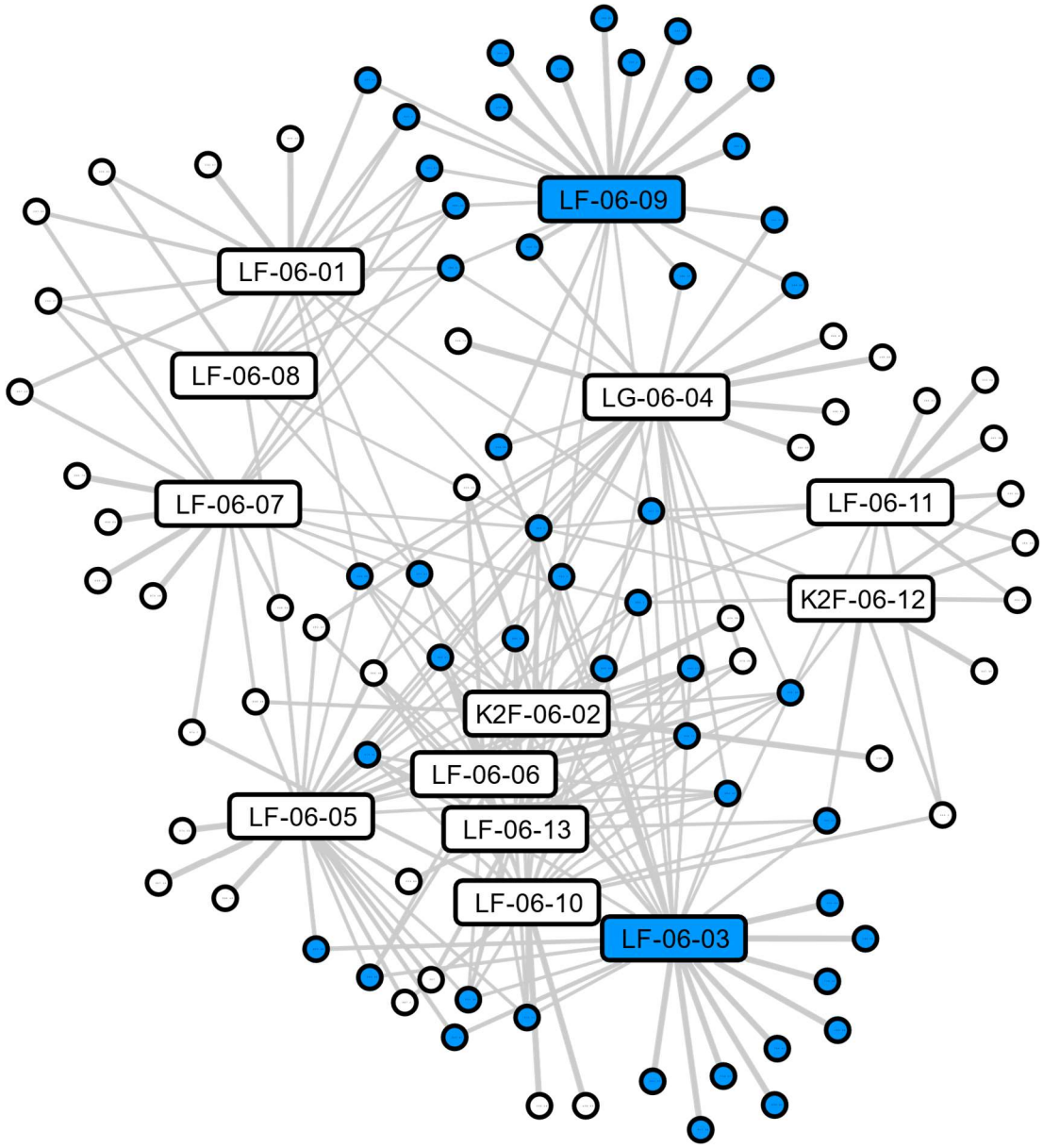

Figure 3.5. MAN of bacteria group 6. Prioritized s and their corresponding metabolite nodes are in blue.

TABLE IV

LIBRARY BACTERIA METADATA

Pseudo-phylogenetic Group	Isolate name	Tissue source	Media type	Plating method	First inoculated on
1	K2G-01-01	Skin	GMF	Undiluted spread	7/18/2019
2	K2G-02-09	Skin	GMF	Stamp	8/12/2019
	K2G-02-10	Skin	GMF	1:100 dilution	8/12/2019
3	K2F-03-21	Skin	SNF	1:100 dilution	7/15/2019
	K2F-03-22	Skin	SNF	Stamp	7/25/2019
4	LF-04-10	Lg. intestine	SNF	Undiluted spread	6/29/2019
	K2G-04-17	Skin	GMF	Stamp	7/12/2019
5	MG-05-21	Sm. intestine	GMF	Undiluted spread	9/7/2019
	K1F-05-03	Skin	SNF	1:100 dilution	7/2/2019
6	LF-06-09	Lg. intestine	SNF	Undiluted spread	6/29/2019
	LF-06-03	Lg. intestine	SNF	Stamp	7/15/2019
7	LF-07-13	Lg. intestine	SNF	Stamp	7/11/2019
	LF-07-13	Lg. intestine	GMF	Undiluted spread	6/29/2019
8	LG-08-03	Lg. intestine	GMF	Stamp	7/3/2019
	LG-08-18	Lg. intestine	GMF	Undiluted spread	7/2/2019
9	K2F-09-16	Skin	SNF	Stamp	7/3/2019
	MF-09-07	Sm. intestine	SNF	Stamp	9/27/2019
10	MF-10-07	Sm. Intestine	SNF	Undiluted spread	7/3/2019
	K2F-10-02	Skin	SNF	Stamp	7/3/2019
11	K1F-11-06	Skin	SNF	1:100 dilution	7/2/2019
	K2F-11-20	Skin	SNF	1:100 dilution	7/25/2019
12	LG-12-11	Lg. intestine	GMF	Stamp	8/30/2019
	LF-12-26	Lg. intestine	SNF	Stamp	7/11/2019

3.3 Conclusions

We innoculated 323 microbial isolates from the tissue of a naked mole rat, and selected a diverse set of 48 isolates to be used as an efficient drug discovery library in the future. In order to find microbial producers of unique metabolites, all of the isolates were screened via MALDI-TOF mass spectrometry to make informed correlations between the isolates' taxonomic and metabolomic profiles. It was discovered that many fungal isolates were not yet separated from bacterial stains, and further analysis will need to be done to select an ideal library before cryopreservation. This is the first reported use of sourcing the microbiome of *H. glaber* for a drug discovery library.

3.4 Experimental

3.4.1 Tissue Preparation

Two 1 cm^2 skin samples were dissected immediately post-mortem from the torso of a 1-year-old male *H. glaber* along with both the small and large intestine by a member of the Thomas Park lab under ACC protocol #18-064. All of the contents of the intestines were left intact. All samples were externally washed with 70% ethanol prior to removal to prevent contamination from the air or interior of the carcass. Each skin sample was added to 5 mL of 1X phosphate-buffered saline (PBS) in a 20 mL conical-bottom centrifuge tube containing 15 sterile 5-mm glass beads. Each half of the intestine was submerged in 30 mL of 1X PBS in a 40 mL conical-bottom centrifuge tube with seven to ten sterile 3-mm glass beads. All four samples were vortexed for approximately 60 seconds.

Figure 3.6 shows photos of each of the tissue samples after bead beating.

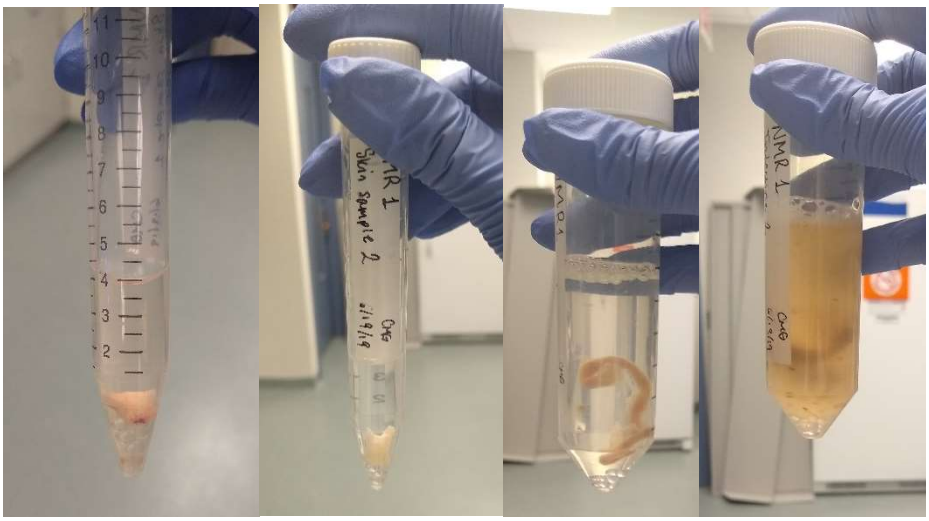

Figure 3.6. The four tissue samples, from left to right: skin, skin, small intestine, large intestine.

3.4.2 Diversity Plate Preparation

Each of the PBS solutions described in "Tissue Preparation" were plated on 24 90-mm Petri dishes containing 20 mL of agar media for a total of 96 diversity plates. Four media types were used, with 3 plating methods, all done in duplicate. The four media types were as follows: GMF (20 g starch, 0.5 g NaCl, 0.01 g $FeSO_4 \cdot 7\ H_2O$, 0.5 g $MgSO_4 \cdot 7H_2O$, 0.5 g K_2HPO_4, 1 g KNO_3, 20 g agar, 1 L Milli-Q water) with 25 mg/L nalidixic acid, GMF with 25 mg/L cycloheximide, SNF+Fiber (20 g Garden of Life Raw Organic Superfood Fiber, 18 g agar, 1 L Milli-Q water) with 25 mg/L nalidixic acid, and SNF+Fiber with 25 mg/L cycloheximide. The PBS solution was plated using serial stamping, an undiluted spread, and a 1:100 dilution spread. The dilution was prepared before any PBS solution was plated, by transferring 100 µL of the tissue homogenate into 10 mL of 1X PBS.

Stamping was done by dipping a sterile swab into the undiluted 1X PBS dilution and lightly dabbing the swab eight times evenly spaced in a circle around the petri dish clockwise

before a final dab in the middle of the plate. For the undiluted and diluted plates, 100 µL of solution was added to the plate and spread. One plate of each media type (GMF + antibiotic, GMF + antifungal, SNF+Fiber + antibiotic, SNF+Fiber + antifungal) was left untreated to act as a media control and monitored for growth along with the other plates.

3.4.3 Microbial Isolation

After nine days, the diversity plates were monitored for growth daily. As distinct colonies formed, the microbes were transferred to 60 mm plates of ISP-2 media (4 g yeast extract powder, 5 g malt extract powder, 4 g dextrose, 15 g agar, 1 L MilliQ water)[29]. Bacteria were transferred via a 10 µL sterile inoculation loop and then quadrant streaked onto a 60 mm agar plate. Fungi were transferred by removing a punch of cells, either by using the back end of a sterile 1 mL pipette tip or by slicing and removing the agar with a sterile 21-gauge sharp needle. The microbes were left to grow on a countertop until growth beyond the inoculation area was observed. If plates appeared to have more than one morphotype, they were re-isolated until pure.

3.4.4 IDBac Sample Preparation

A sterile toothpick was used to sample either a single bacterial colony or approximately a 4 mm^2 area of a fungal colony and transfer to a 2 mL Eppendorf tube with 5 µL of HPLC grade trifluoroacetic acid (TFA). The cells were left to lyse for 30 minutes before the addition of 20 µL of HPLC grade acetonitrile (ACN) and 15 µL of MilliQ water. The cells were then vortexed for 10 seconds before being centrifuged at 10,000 rpm for 2 minutes. The resulting supernatant (2 µL) was mixed by pipette with 2 µL of recrystallized 10 mg/mL CHCA matrix[27]. Three technical replicates of 1 µL each were then spotted on a ground steel 396 target plate for analysis in both

positive linear and reflectron modes on an Autoflex Speed LRF mass spectrometer (Bruker Daltonics) equipped with a smartbeam-II laser (355 nm).

3.4.5 MALDI-TOF-MS Sample Acquisition

Samples were collected via AutoXecute methods hosted at DOI: 10.5281/zenodo.1115619. Laser size was set to 3-medium. Laser power for reflectron and linear mode was between 40-70%. Gain for reflectron mode was within 9.0x to 12.0x, and gain for linear mode ranged from 10.0x to 20.0x based on optimization after instrument maintenance. Reflectron mode was calibrated with Peptide Calibration Mix (Bruker Daltonics) and linear mode was calibrated with Protein Calibration Standard I (Bruker Daltonics).

3.4.6 IDBac Parameters

Bacteria Dendrogram: The dendrogram in Figure 3.4 was created by analyzing 273 samples and retaining peaks with a signal to noise ratio above 3.5 and occurring in greater than 70 % of replicate spectra (two of three replicates). Peaks occurring below 2001 *m/z* or above 15000 *m/z* were removed from the analyses. For clustering spectra, cosine distance and average (unweighted pair group method with arithmetic mean) algorithms were used.

Bacteria MANs: These MANs were created by subtracting a matrix blank, retaining peaks with a signal to noise ratio above 4, and occurring in greater than 70% of replicate spectra (two of three replicates). Peaks occurring below 200 m/z or above 2000 m/z were removed from the analysis.

Fungi Dendrogram: The dendrogram in Figure 3.2 was created by analyzing 50 samples and retaining peaks with a signal to noise ratio above 4.5 and occurring in greater than 60 % of

replicate spectra (one of three replicates). Peaks occurring below 2001 *m/z* or above 15000 *m/z* were removed from the analyses. For clustering spectra, cosine distance and average (UPGMA) algorithms were used.

Fungi MAN: This MAN was created by analyzing 50 samples, subtracting a matrix blank, retaining peaks with a signal to noise ratio above 4.5, and occurring in greater than 70% of replicate spectra (two of three replicates). Peaks occurring below 200 m/z or above 2000 m/z were removed from the analysis.

3.4.7 MassIVE Dataset

The full MALDI-TOF-MS dataset can be accessed at MassIVE accession number MSV000085215.

3.5 Cited Literature

(1) Ruby, J. G.; Smith, M.; Buffenstein, R. Naked Mole-Rat Mortality Rates Defy Gompertzian Laws by Not Increasing with Age. *eLife* **2018**, *7*, e31157. https://doi.org/10.7554/eLife.31157.

(2) Buffenstein, R. The Naked Mole Rat--A New Record for the Oldest Living Rodent. *Sci. Aging Knowl. Environ.* **2002**, *2002* (21), 7pe–7. https://doi.org/10.1126/sageke.2002.21.pe7.

(3) Ivy, C. M.; Sprenger, R. J.; Bennett, N. C.; Jaarsveld, B.; Hart, D. W.; Kirby, A. M.; Yaghoubi, D.; Storey, K. B.; Milsom, W. K.; Pamenter, M. E. The Hypoxia Tolerance of Eight Related African Mole-rat Species Rivals That of Naked Mole-rats, despite Divergent Ventilatory and Metabolic Strategies in Severe Hypoxia. *Acta Physiol.* **2020**. https://doi.org/10.1111/apha.13436.

(4) Kirby, A. M.; Fairman, G. D.; Pamenter, M. E. Atypical Behavioural, Metabolic and Thermoregulatory Responses to Hypoxia in the Naked Mole Rat (Heterocephalus Glaber). *J. Zool.* **2018**, *305* (2), 106–115. https://doi.org/10.1111/jzo.12542.

(5) Park, T. J.; Lu, Y.; Jüttner, R.; Smith, E. S. J.; Hu, J.; Brand, A.; Wetzel, C.; Milenkovic, N.; Erdmann, B.; Heppenstall, P. A.; Laurito, C. E.; Wilson, S. P.; Lewin, G. R. Selective

Inflammatory Pain Insensitivity in the African Naked Mole-Rat (Heterocephalus Glaber). *PLoS Biol.* **2008**, *6* (1), e13. https://doi.org/10.1371/journal.pbio.0060013.

(6) Tian, X.; Azpurua, J.; Hine, C.; Vaidya, A.; Myakishev-Rempel, M.; Ablaeva, J.; Mao, Z.; Nevo, E.; Gorbunova, V.; Seluanov, A. High-Molecular-Mass Hyaluronan Mediates the Cancer Resistance of the Naked Mole Rat. *Nature* **2013**, *499* (7458), 346–349. https://doi.org/10.1038/nature12234.

(7) Manskikh, V. N.; Averina, O. A.; Nikiforova, A. I. Spontaneous and Experimentally Induced Pathologies in the Naked Mole Rat (Heterocephalus Glaber). *Biochemistry* **2017**, *82* (12), 1504–1512.

(8) von Salm, J. L.; Witowski, C. G.; Demers, D. H.; Young, R. M.; Calcul, L.; Baker, B. J. Screening Marine Microbial Libraries. In *Marine Biomedicine: From Beach to Bedside*; CRC Press: Boca Raton, 2016; pp 105–127.

(9) Cheuka, P.; Mayoka, G.; Mutai, P.; Chibale, K. The Role of Natural Products in Drug Discovery and Development against Neglected Tropical Diseases. *Molecules* **2016**, *22* (1), 58. https://doi.org/10.3390/molecules22010058.

(10) Wright, G. D. Opportunities for Natural Products in 21st Century Antibiotic Discovery. *Nat. Prod. Rep.* **2017**, *34* (7), 694–701. https://doi.org/10.1039/C7NP00019G.

(11) Sharon, G.; Garg, N.; Debelius, J.; Knight, R.; Dorrestein, P. C.; Mazmanian, S. K. Specialized Metabolites from the Microbiome in Health and Disease. *Cell Metab.* **2014**, *20* (5), 719–730. https://doi.org/10.1016/j.cmet.2014.10.016.

(12) Wilson, M. R.; Zha, L.; Balskus, E. P. Natural Product Discovery from the Human Microbiome. *J. Biol. Chem.* **2017**, *292* (21), 8546–8552. https://doi.org/10.1074/jbc.R116.762906.

(13) Ochoa, J. L.; Sanchez, L. M.; Koo, B.-M.; Doherty, J. S.; Rajendram, M.; Huang, K. C.; Gross, C. A.; Linington, R. G. Marine Mammal Microbiota Yields Novel Antibiotic with Potent Activity Against Clostridium Difficile. *ACS Infect. Dis.* **2018**, *4* (1), 59–67. https://doi.org/10.1021/acsinfecdis.7b00105.

(14) Sanchez, L. M.; Wong, W. R.; Riener, R. M.; Schulze, C. J.; Linington, R. G. Examining the Fish Microbiome: Vertebrate-Derived Bacteria as an Environmental Niche for the Discovery of Unique Marine Natural Products. *PLoS ONE* **2012**, *7* (5), e35398. https://doi.org/10.1371/journal.pone.0035398.

(15) Sanchez, L. M.; Cheng, A. T.; Warner, C. J. A.; Townsley, L.; Peach, K. C.; Navarro, G.; Shikuma, N. J.; Bray, W. M.; Riener, R. M.; Yildiz, F. H.; Linington, R. G. Biofilm Formation and Detachment in Gram-Negative Pathogens Is Modulated by Select Bile Acids. *PLOS ONE* **2016**, *11* (3), e0149603. https://doi.org/10.1371/journal.pone.0149603.

(16) Motley, J. L.; Stamps, B. W.; Mitchell, C. A.; Thompson, A. T.; Cross, J.; You, J.; Powell, D. R.; Stevenson, B. S.; Cichewicz, R. H. Opportunistic Sampling of Roadkill as an Entry Point to Accessing Natural Products Assembled by Bacteria Associated with Non-Anthropoidal Mammalian Microbiomes. *J. Nat. Prod.* **2017**, *80* (3), 598–608. https://doi.org/10.1021/acs.jnatprod.6b00772.

(17) Debebe, T.; Biagi, E.; Soverini, M.; Holtze, S.; Hildebrandt, T. B.; Birkemeyer, C.; Wyohannis, D.; Lemma, A.; Brigidi, P.; Savkovic, V.; König, B.; Candela, M.; Birkenmeier, G. Unraveling the Gut Microbiome of the Long-Lived Naked Mole-Rat. *Sci Rep* **2017**, *7* (1), 9590.

(18) Hills, R. D.; Pontefract, B. A.; Mishcon, H. R.; Black, C. A.; Sutton, S. C.; Theberge, C. R. Gut Microbiome: Profound Implications for Diet and Disease. *Nutrients* **2019**, *11* (7). https://doi.org/10.3390/nu11071613.

(19) Requena, T.; Martínez-Cuesta, M. C.; Peláez, C. Diet and Microbiota Linked in Health and Disease. *Food Funct.* **2018**, *9* (2), 688–704. https://doi.org/10.1039/C7FO01820G.

(20) Fischbach, M. A. Microbiome: Focus on Causation and Mechanism. *Cell* **2018**, *174* (4), 785–790. https://doi.org/10.1016/j.cell.2018.07.038.

(21) Deacon, J. W. Fungal Nutrition. In *Fungal biology*; Blackwell Pub: Malden, MA, 2006; pp 110–121.

(22) Condren, A. R.; Costa, M. S.; Sanchez, N. R.; Konkapaka, S.; Gallik, K. L.; Saxena, A.; Murphy, B. T.; Sanchez, L. M. *Addition of Insoluble Fiber to Isolation Media Allows for Increased Metabolite Diversity of Lab-Cultivable Microbes Derived from Zebrafish Gut Samples*; preprint; Microbiology, 2019. https://doi.org/10.1101/854109.

(23) Ivantiskaya, L. P.; Singal, S. M.; Bibikova, M. V.; Vostrov, S. N. Direct Isolation of Micromonospora on Selective Media with Gentamicin. *Antibiotiki* **1978**, *23*, 690–692.

(24) Clark, C. M.; Costa, M. S.; Sanchez, L. M.; Murphy, B. T. Coupling MALDI-TOF Mass Spectrometry Protein and Specialized Metabolite Analyses to Rapidly Discriminate Bacterial Function. *Proc. Natl. Acad. Sci.* **2018**, *115* (19), 4981–4986. https://doi.org/10.1073/pnas.1801247115.

(25) Cleary, J. L.; Kolachina, S.; Wolfe, B. E.; Sanchez, L. M. Coproporphyrin III Produced by the Bacterium *Glutamicibacter Arilaitensis* Binds Zinc and Is Upregulated by Fungi in Cheese Rinds. *mSystems* **2018**, *3* (4), e00036-18, /msystems/3/4/msys.00036-18.atom. https://doi.org/10.1128/mSystems.00036-18.

(26) Siddiqui, M. S.; Thodey, K.; Trenchard, I.; Smolke, C. D. Advancing Secondary Metabolite Biosynthesis in Yeast with Synthetic Biology Tools. *FEMS Yeast Res.* **2012**, *12* (2), 144–170. https://doi.org/10.1111/j.1567-1364.2011.00774.x.

(27) Freiwald, A.; Sauer, S. Phylogenetic Classification and Identification of Bacteria by Mass Spectrometry. *Nat. Protoc.* **2009**, *4* (5), 732–742. https://doi.org/10.1038/nprot.2009.37.

(28) Costa, M. S.; Clark, C. M.; Ómarsdóttir, S.; Sanchez, L. M.; Murphy, B. T. Minimizing Taxonomic and Natural Product Redundancy in Microbial Libraries Using MALDI-TOF MS and the Bioinformatics Pipeline IDBac. *J. Nat. Prod.* **2019**, *82* (8), 2167–2173. https://doi.org/10.1021/acs.jnatprod.9b00168.

(29) Shirling, E. B.; Gottlieb, D. Methods for Characterization of Streptomyces Species. *Int. J. Syst. Bacteriol.* **1966**, *16* (3), 313–340. https://doi.org/10.1099/00207713-16-3-313.

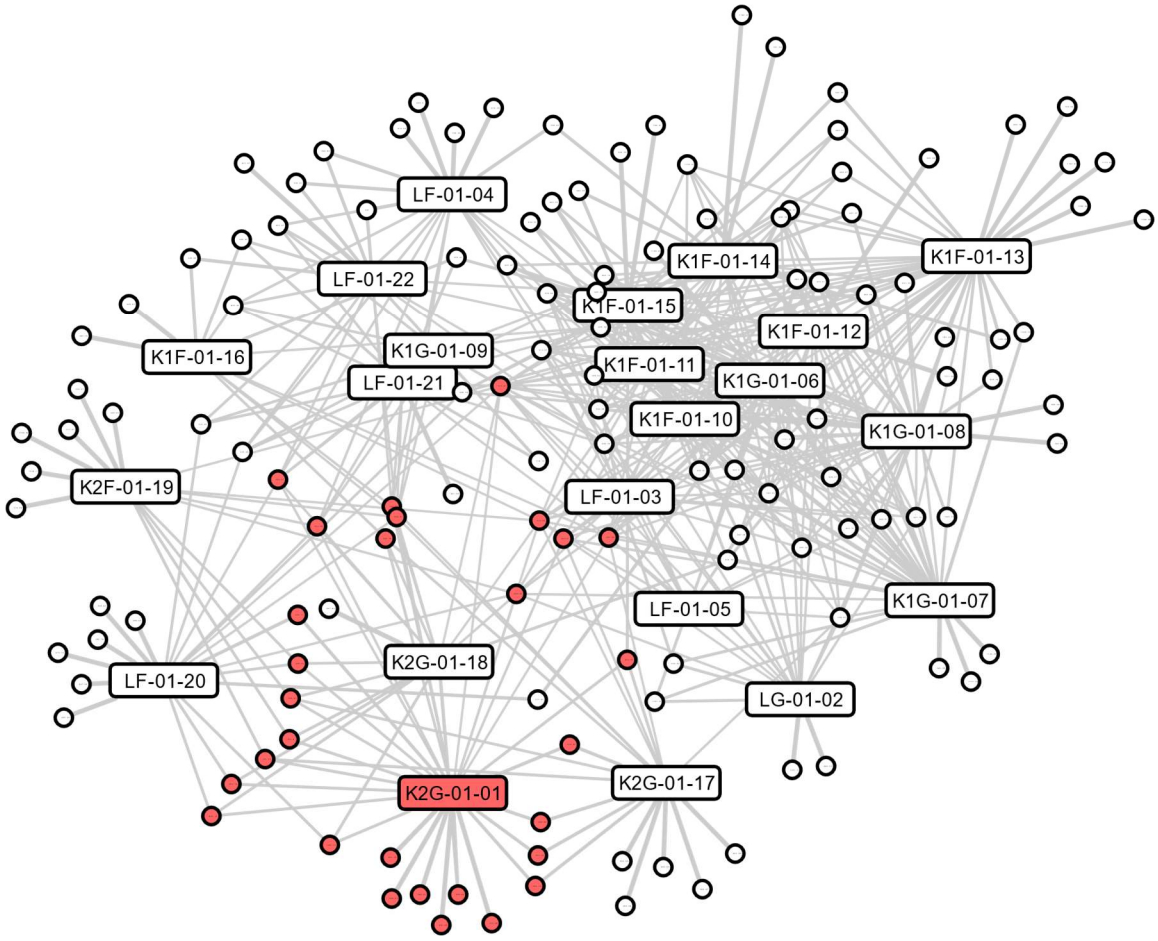

Figure A.1 MAN of bacteria group 1. Chosen strains are highlighted in red.

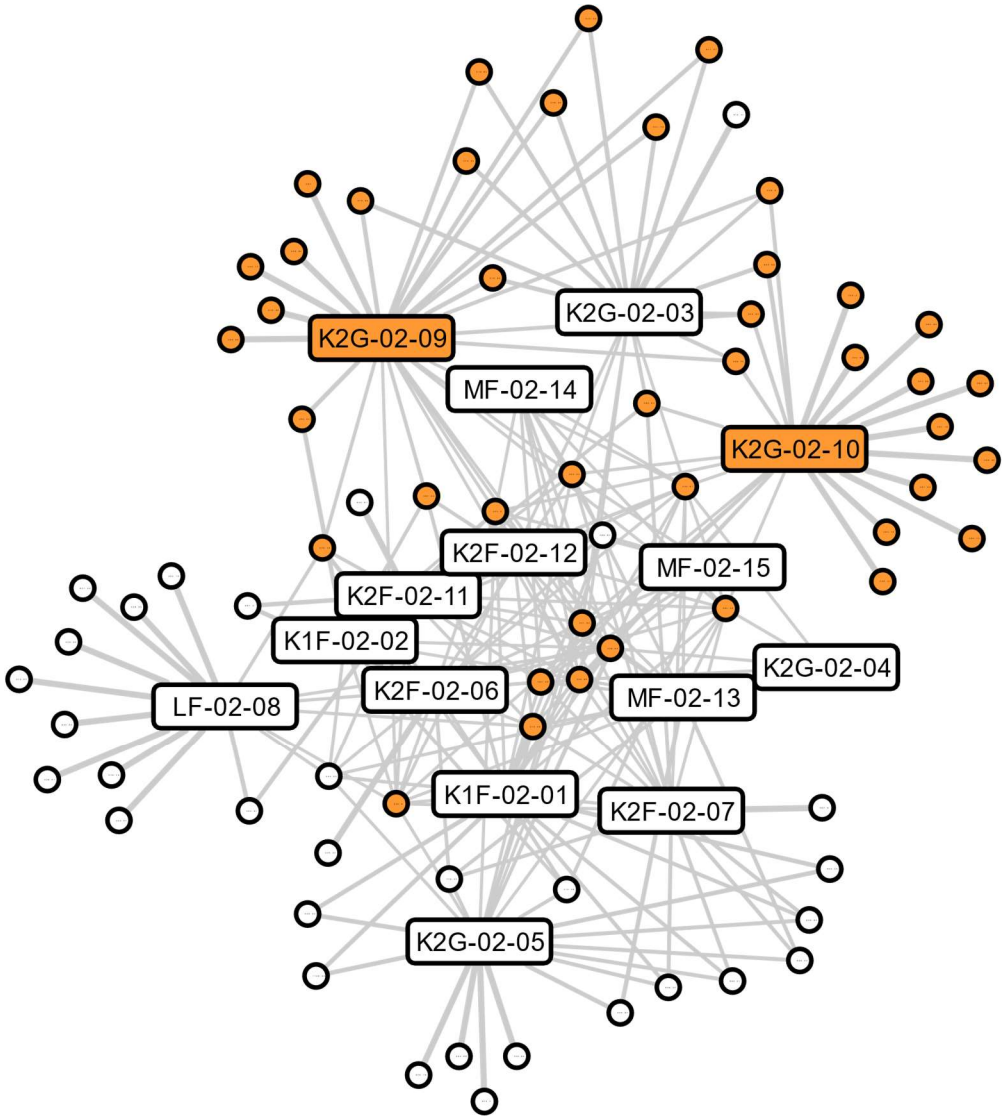

Figure A.2 MAN of bacteria group 2. Chosen strains are highlighted in orange.

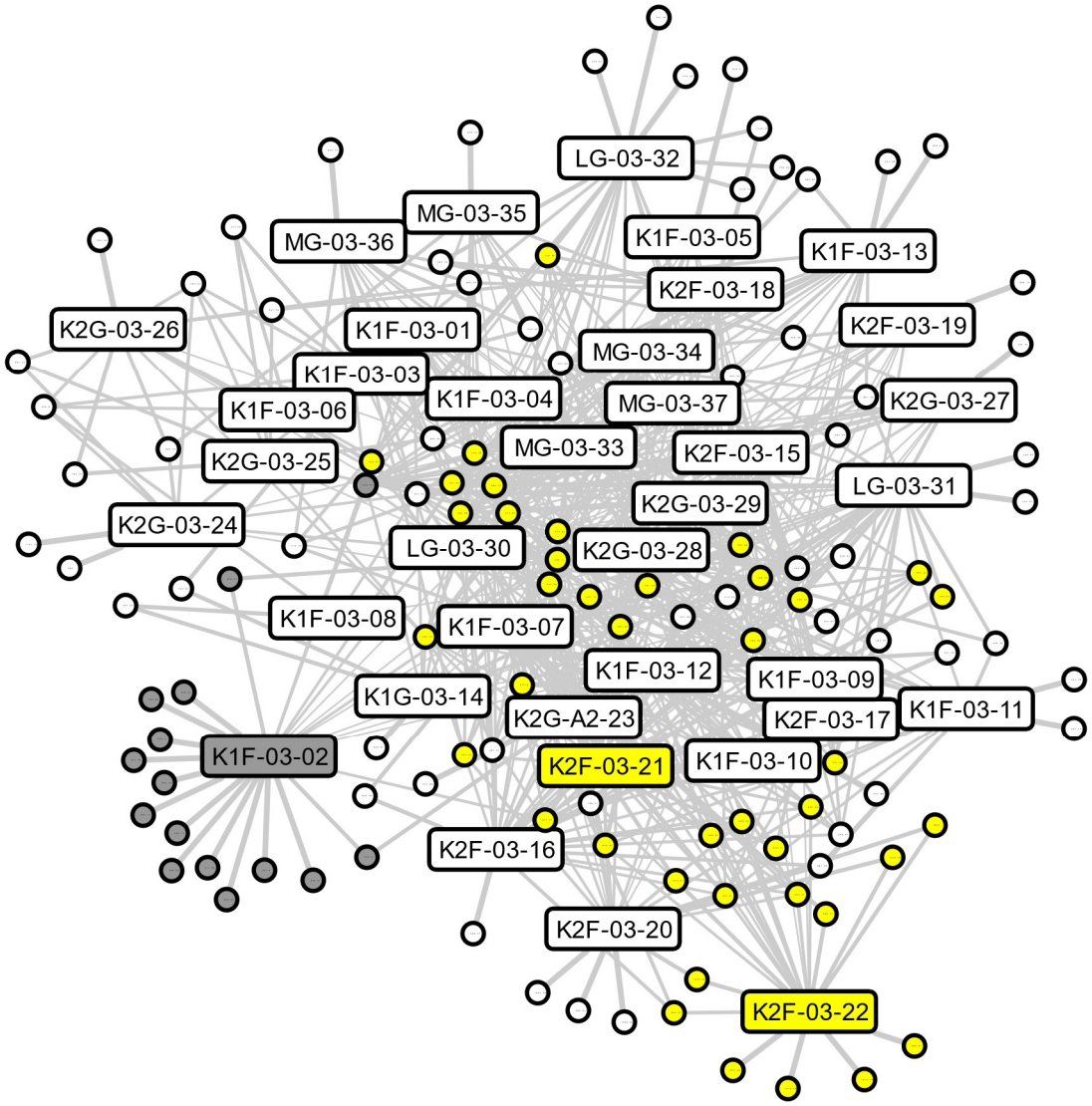

Figure A.3 MAN of bacteria group 3. Chosen strains are highlighted in yellow. Gray marks a chosen strain that failed to grow in liquid media and was discarded.

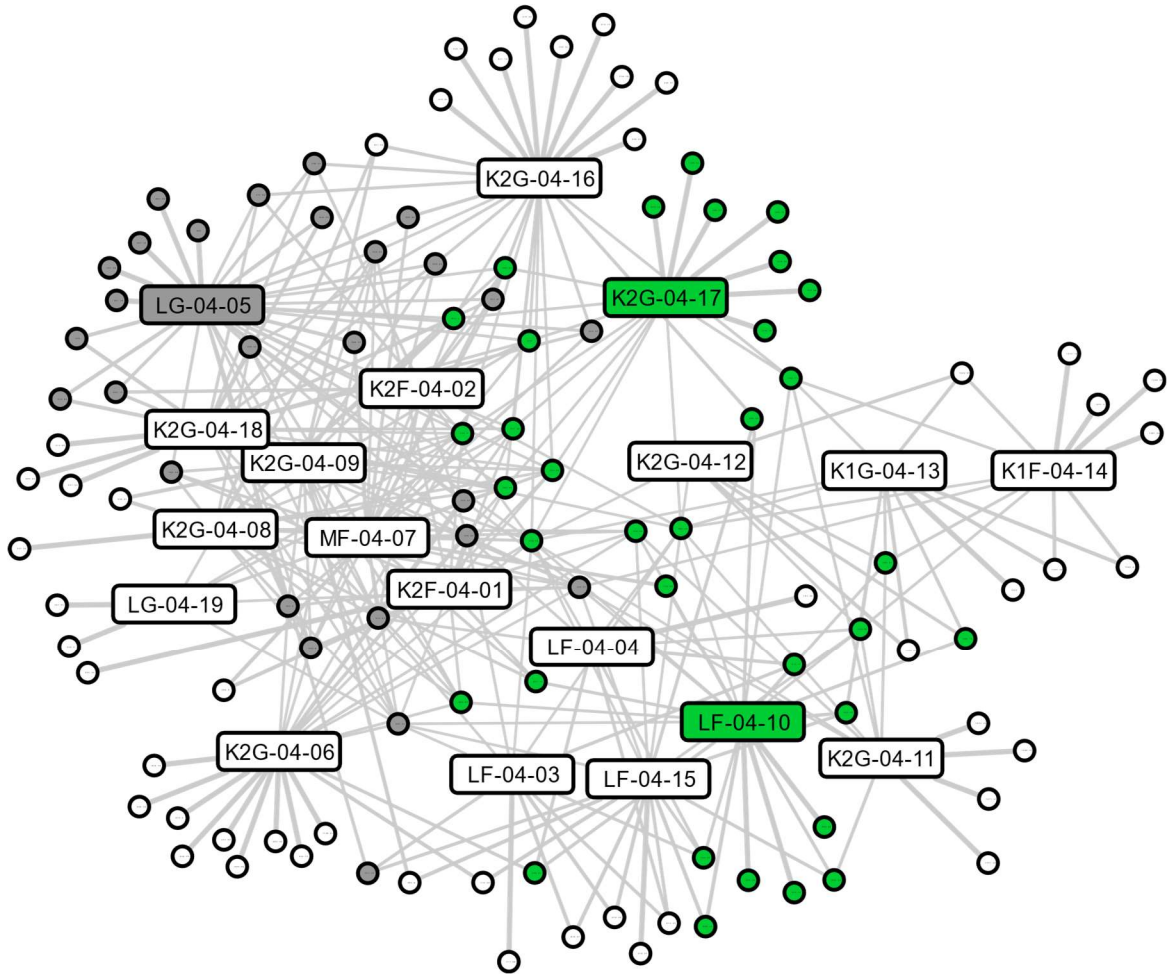

Figure A.4 MAN of bacteria group 4. Chosen strains are highlighted in green. Gray marks a chosen strain that failed to grow in liquid media and was discarded.

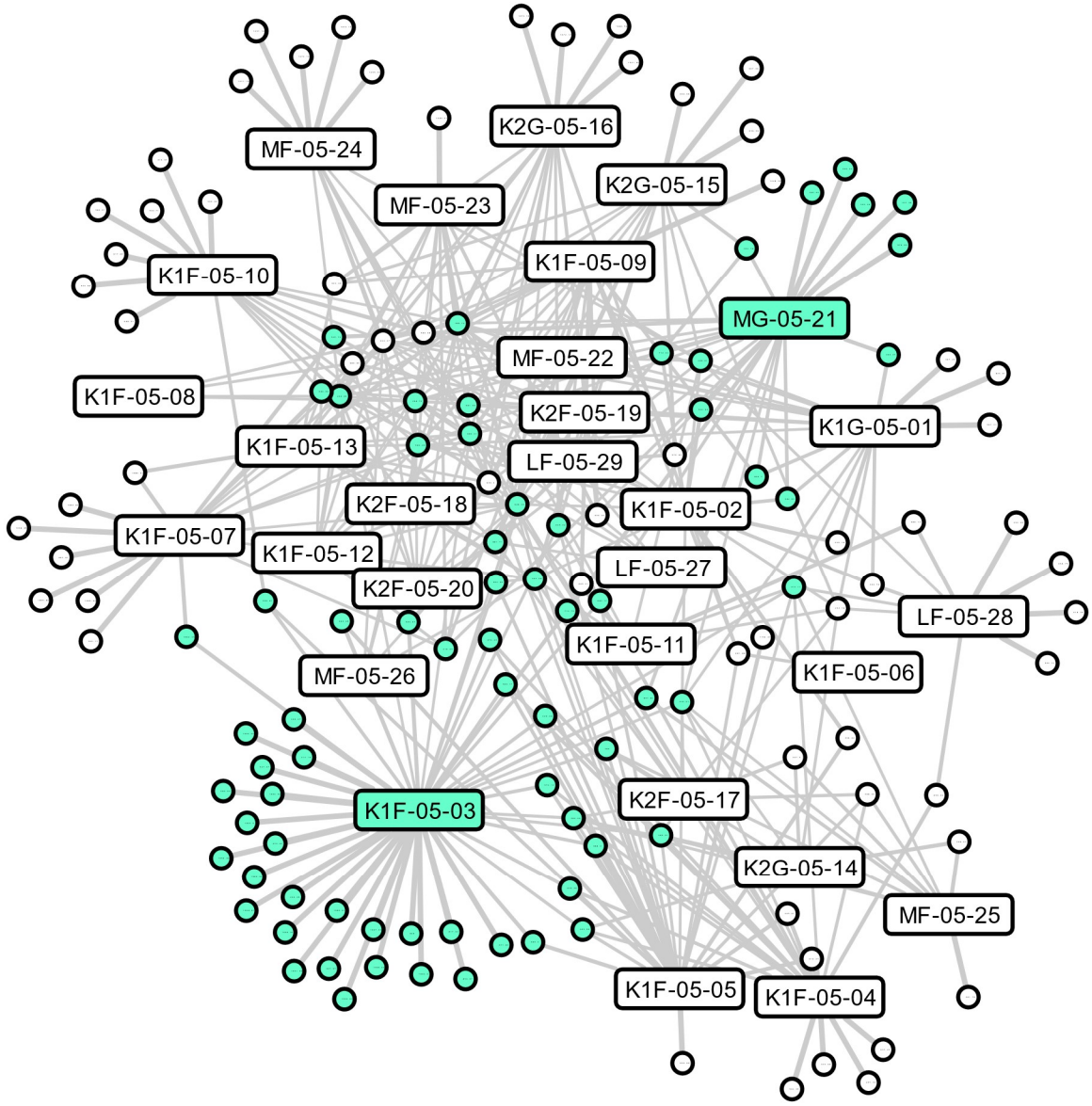

Figure A.5 MAN of bacteria group 5. Chosen strains are highlighted in cyan.

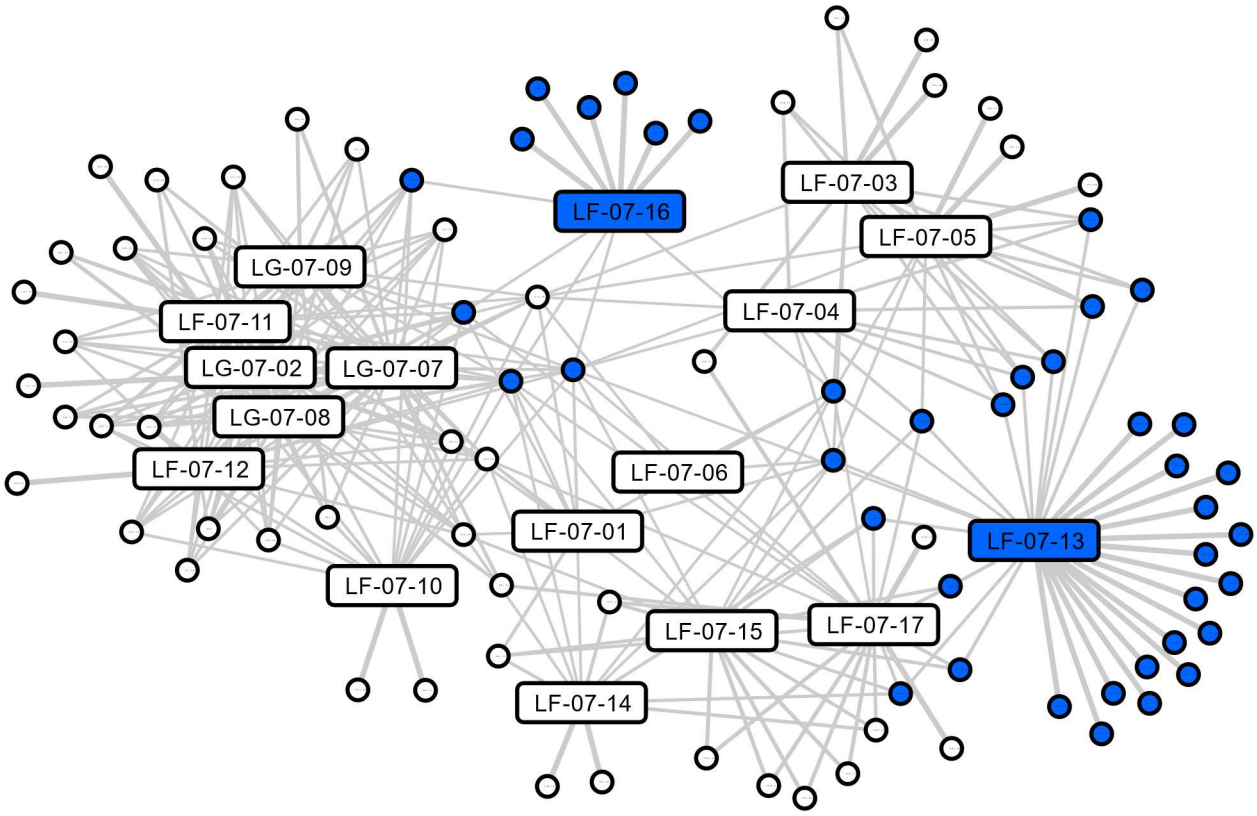

Figure A.6 MAN of bacteria group 7. Chosen strains are highlighted in blue.

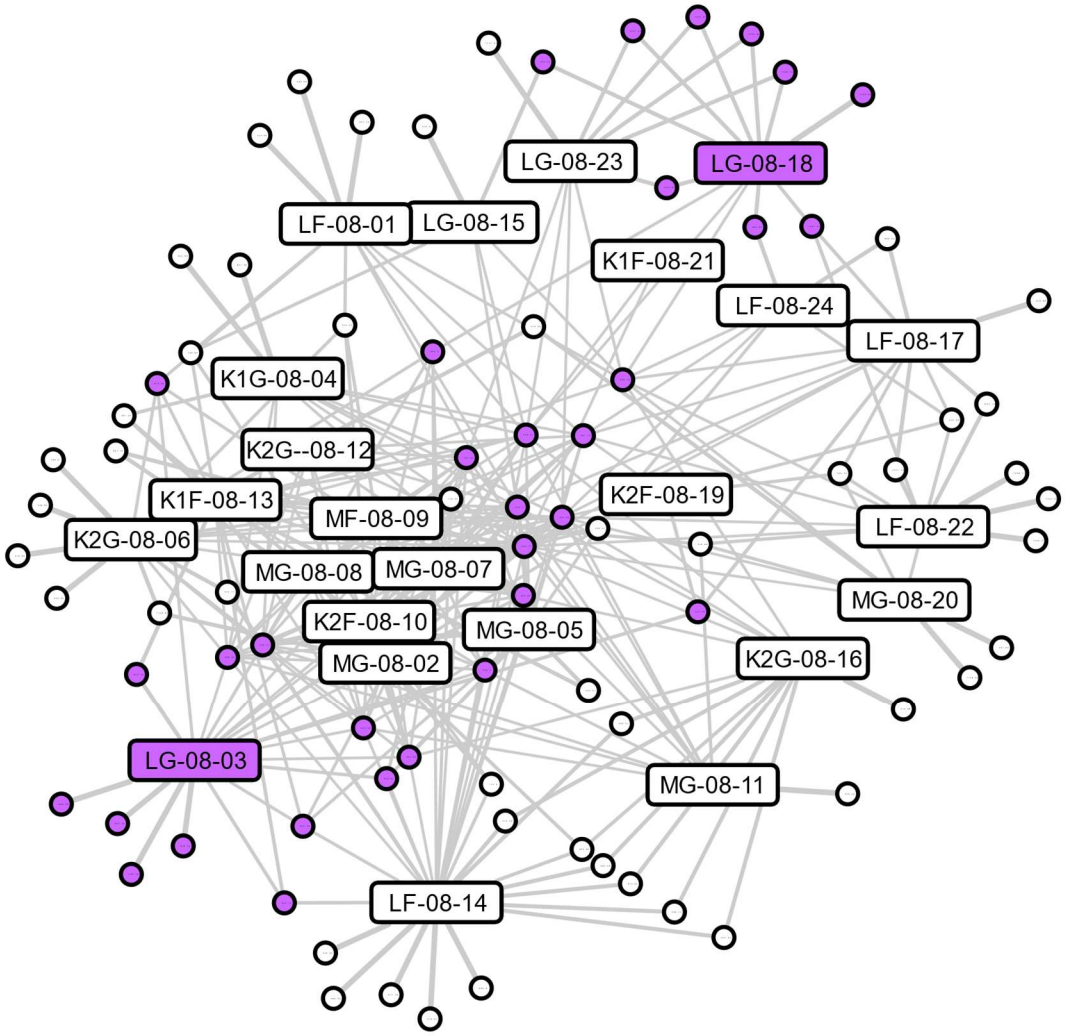

Figure A.7 MAN of bacteria group 8. Chosen strains are highlighted in purple.

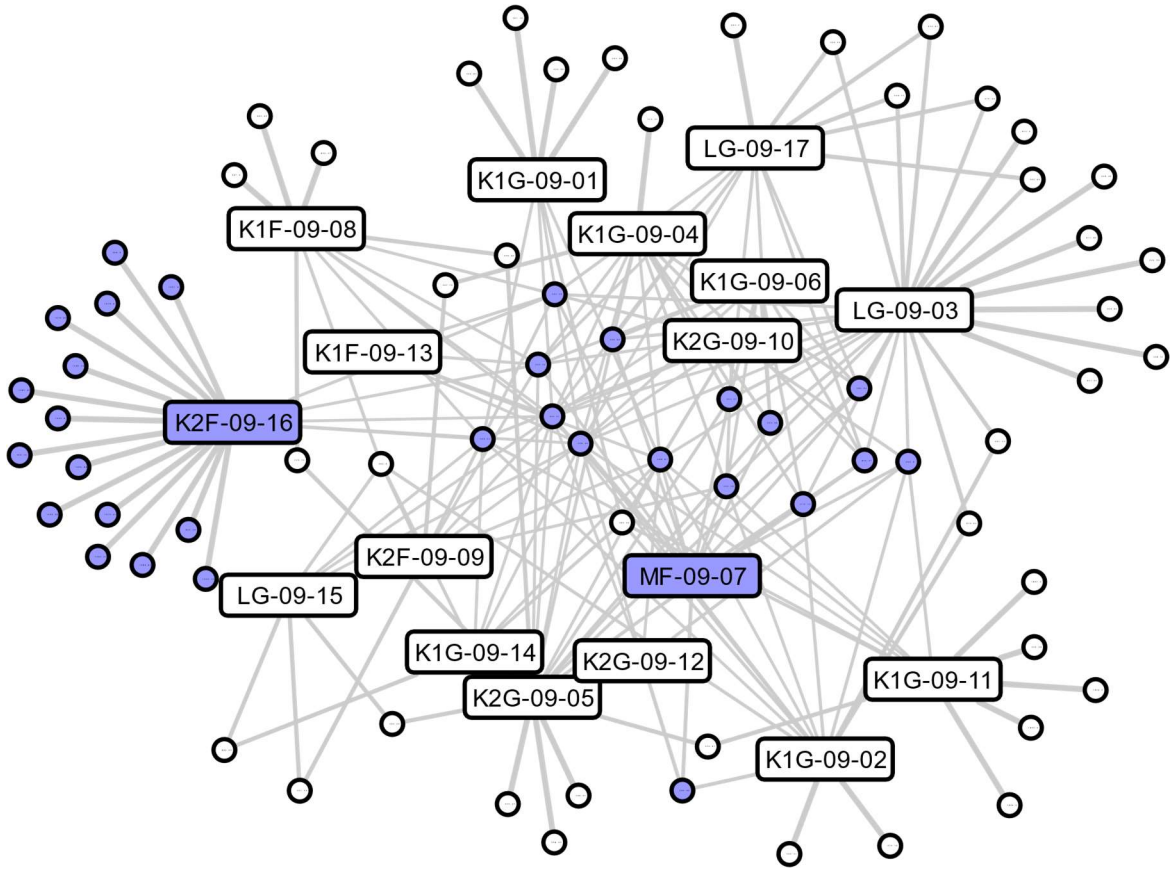

Figure A.8 MAN of bacteria group 9. Chosen strains are highlighted in periwinkle.

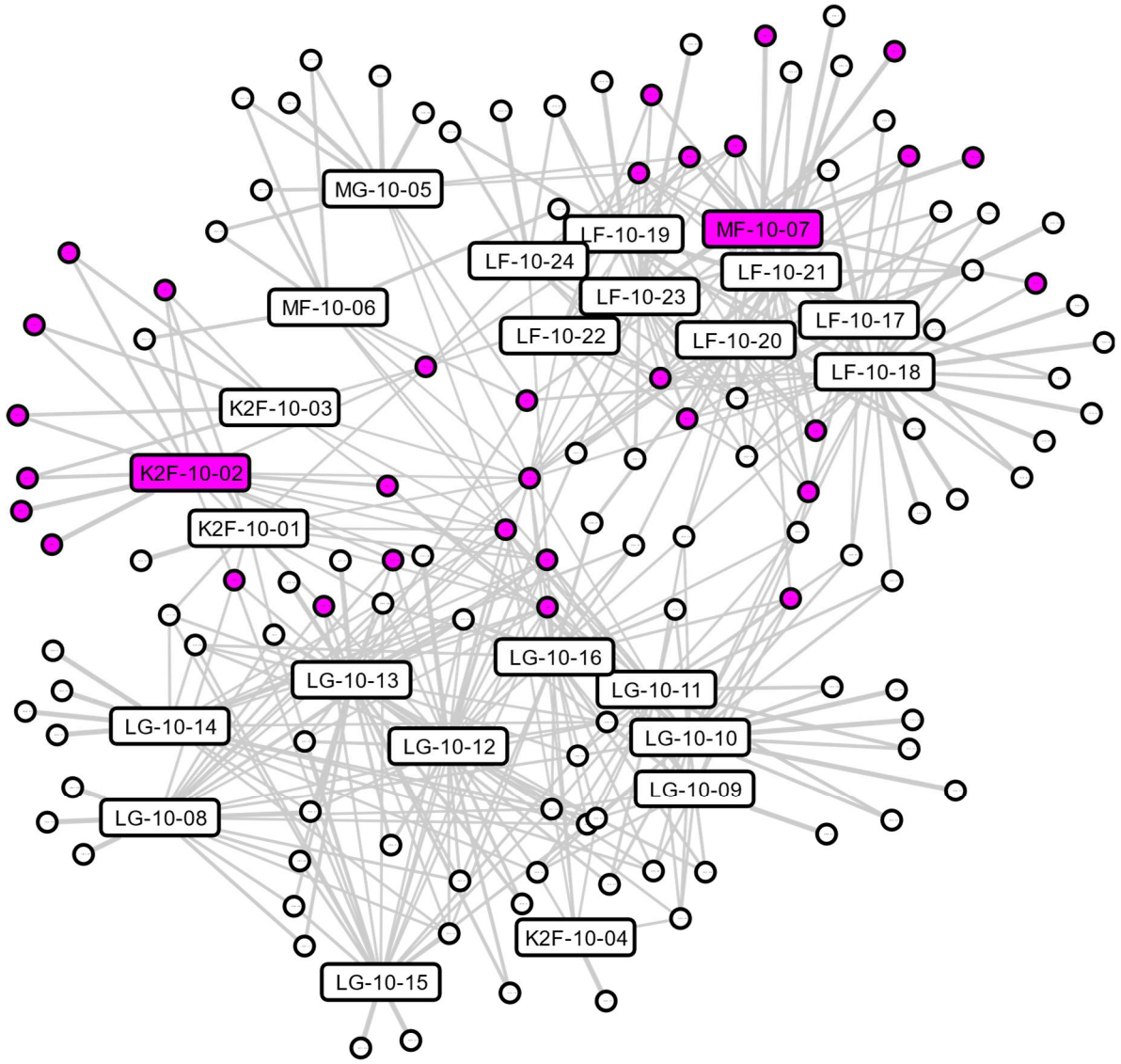

Figure A.9 MAN of bacteria group 10. Chosen strains are highlighted in magenta.

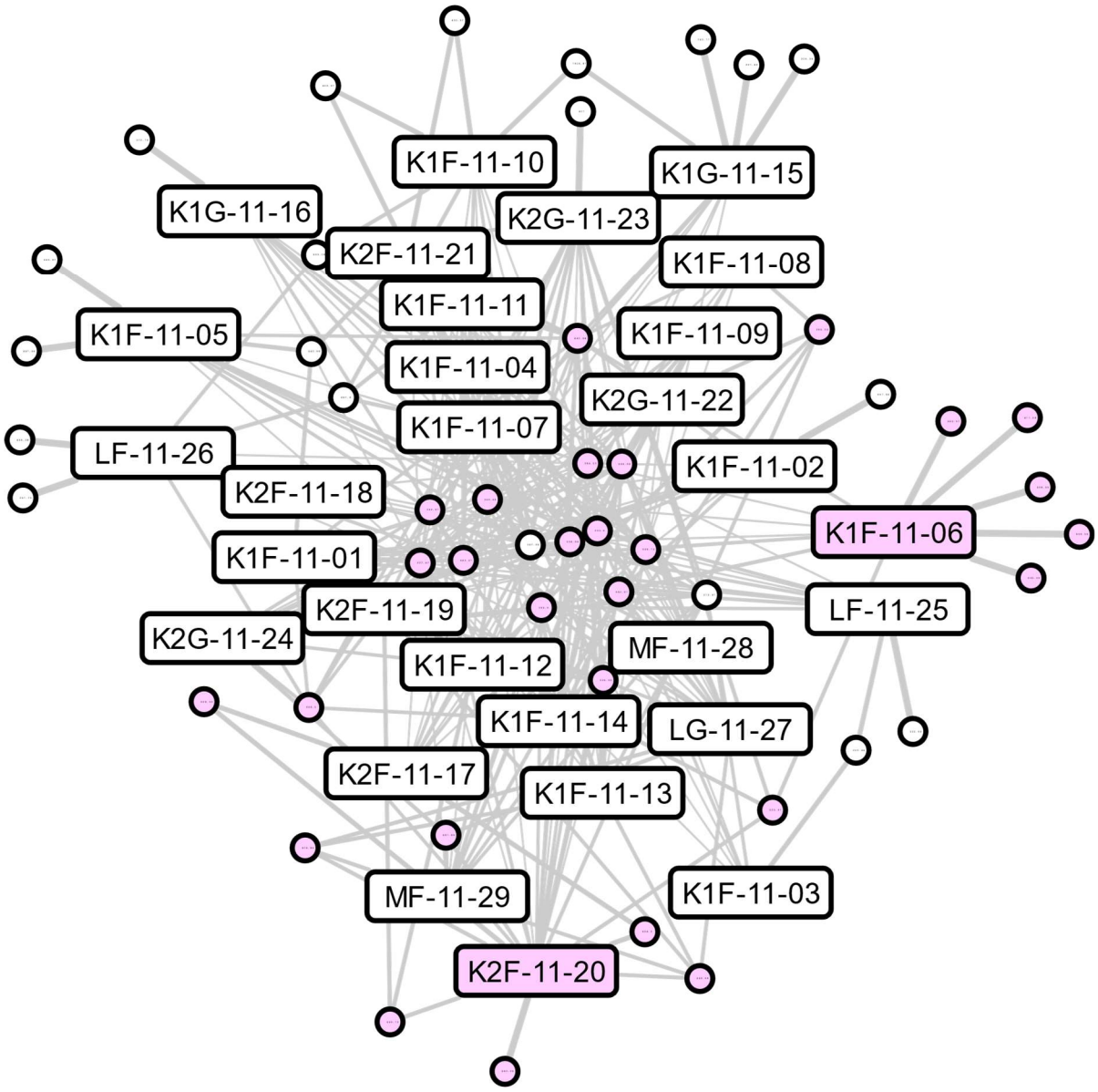

Figure A.10 MAN of bacteria group 11. Chosen strains are highlighted in pink.

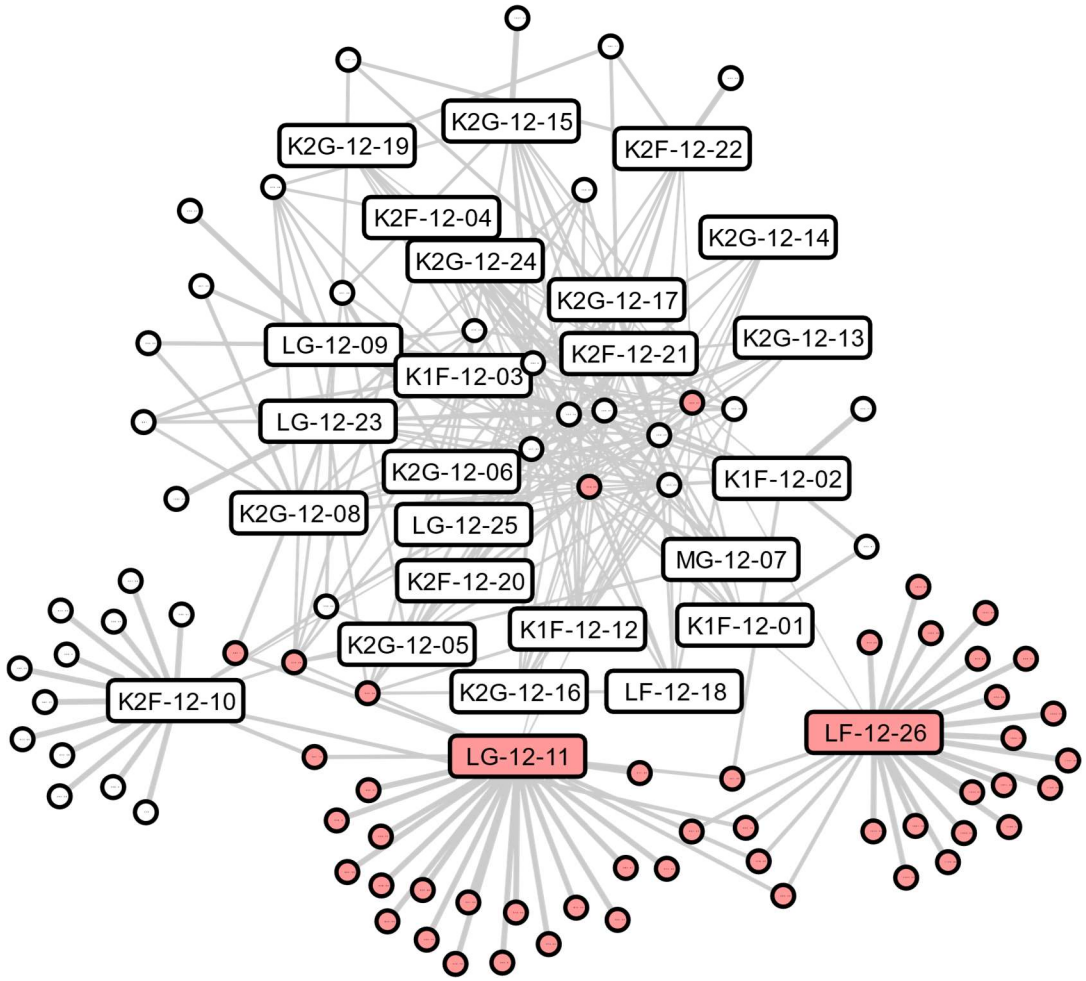

Figure A.11 MAN of bacteria group 12. Chosen strains are highlighted in pink.

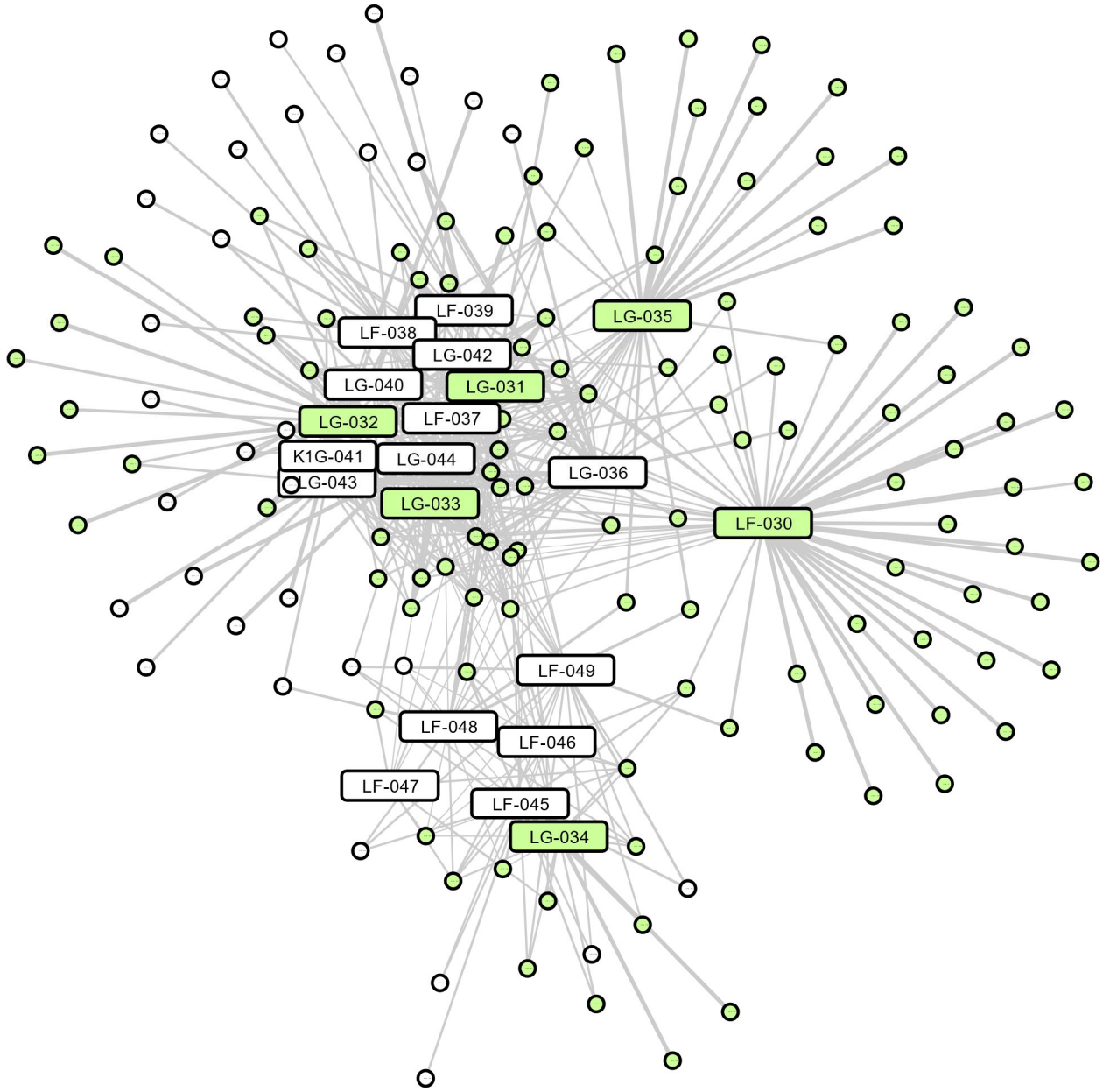

Figure A.12 MAN of Fungi group A. colored notes indicate library strains.

APPENDIX B. OXFORD UNIVERSITY PRESS LICENSE

OXFORD UNIVERSITY PRESS LICENSE TERMS AND CONDITIONS

Feb 24, 2020

This Agreement between University of Illinois at Chicago -- Cynthia Grim ("You") and Oxford University Press ("Oxford University Press") consists of your license details and the terms and conditions provided by Oxford University Press and Copyright Clearance Center.

License Number	4771191161723
License date	Feb 17, 2020
Licensed Content Publisher	Oxford University Press
Licensed Content Publication	FEMS Microbiology Letters
Licensed Content Title	Staring into the void: demystifying microbial metabolomics
Licensed Content Author	Grim, Cynthia M; Luu, Gordon T
Licensed Content Date	Jun 18, 2019
Type of Use	Thesis/Dissertation
Institution name	
Title of your work	Using Mass Spectrometry to Quantitate and Analyze Bioactive Small Molecules
Publisher of your work	University of Illinois at Chicago
Expected publication date	Mar 2020
Permissions cost	0.00 USD
Value added tax	0.00 USD
Total	**0.00 USD**
Title	Using Mass Spectrometry to Quantitate and Analyze Bioactive Small Molecules
Institution name	University of Illinois at Chicago
Expected presentation date	Mar 2020
Portions	Adapted version of figure 1, Analytical Techniques, Fluxomics, Global Natural Products Social Molecular Networking, In silico annotation
Requestor Location	[redacted] CHICAGO, IL 60607 United States Attn: University of Illinois at Chicago
Publisher Tax ID	GB125506730
Total	**0.00 USD**
Terms and Conditions	

STANDARD TERMS AND CONDITIONS FOR REPRODUCTION OF MATERIAL FROM AN OXFORD UNIVERSITY PRESS JOURNAL

1. Use of the material is restricted to the type of use specified in your order details.
2. This permission covers the use of the material in the English language in the following territory: world. If you have requested additional permission to translate this material, the terms and conditions of this reuse will be set out in clause 12.
3. This permission is limited to the particular use authorized in (1) above and does not allow you to sanction its use elsewhere in any other format other than specified above, nor does it apply to quotations, images, artistic works etc that have been reproduced from other sources which may be part of the material to be used.
4. No alteration, omission or addition is made to the material without our written consent. Permission must be re-cleared with Oxford University Press if/when you decide to reprint.

5. The following credit line appears wherever the material is used: author, title, journal, year, volume, issue number, pagination, by permission of Oxford University Press or the sponsoring society if the journal is a society journal. Where a journal is being published on behalf of a learned society, the details of that society must be included in the credit line.
6. For the reproduction of a full article from an Oxford University Press journal for whatever purpose, the corresponding author of the material concerned should be informed of the proposed use. Contact details for the corresponding authors of all Oxford University Press journal contact can be found alongside either the abstract or full text of the article concerned, accessible from www.oxfordjournals.org Should there be a problem clearing these rights, please contact journals.permissions@oup.com
7. If the credit line or acknowledgement in our publication indicates that any of the figures, images or photos was reproduced, drawn or modified from an earlier source it will be necessary for you to clear this permission with the original publisher as well. If this permission has not been obtained, please note that this material cannot be included in your publication/photocopies.
8. While you may exercise the rights licensed immediately upon issuance of the license at the end of the licensing process for the transaction, provided that you have disclosed complete and accurate details of your proposed use, no license is finally effective unless and until full payment is received from you (either by Oxford University Press or by Copyright Clearance Center (CCC)) as provided in CCC's Billing and Payment terms and conditions. If full payment is not received on a timely basis, then any license preliminarily granted shall be deemed automatically revoked and shall be void as if never granted. Further, in the event that you breach any of these terms and conditions or any of CCC's Billing and Payment terms and conditions, the license is automatically revoked and shall be void as if never granted. Use of materials as described in a revoked license, as well as any use of the materials beyond the scope of an unrevoked license, may constitute copyright infringement and Oxford University Press reserves the right to take any and all action to protect its copyright in the materials.
9. This license is personal to you and may not be sublicensed, assigned or transferred by you to any other person without Oxford University Press's written permission.
10. Oxford University Press reserves all rights not specifically granted in the combination of (i) the license details provided by you and accepted in the course of this licensing transaction, (ii) these terms and conditions and (iii) CCC's Billing and Payment terms and conditions.
11. You hereby indemnify and agree to hold harmless Oxford University Press and CCC, and their respective officers, directors, employs and agents, from and against any and all claims arising out of your use of the licensed material other than as specifically authorized pursuant to this license.
12. Other Terms and Conditions:
v1.4

Questions? customercare@copyright.com or +1-855-239-3415 (toll free in the US) or +1-978-646-2777.

VITA

Cynthia M. Grim

Chicago, IL – grim.cynthia@gmail.com

Education

University of Illinois at Chicago, Chicago, IL 2018 – Current

M.S. student in Pharmacognosy

University of South Florida, Tampa, FL 2013 – 2017

B.S. Chemical Engineering

Minor in Chemistry

Research Experience

Graduate Assistant, UIC 2019 – Current

Department of Pharmaceutical Sciences

Thesis: Using Mass Spectrometry to Quantitate and Analyze Bioactive Small Molecules

Advisor: Dr. Laura Sanchez

Undergraduate Researcher, USF 2013 – 2017

Department of Chemistry

Thesis: Chemical Study of *Aiolochroia crassa*

Advisor: Dr. Bill Baker

Publications

---

1. **Cynthia M Grim***, Gordon T Luu*, Laura M Sanchez, Staring into the void: demystifying microbial metabolomics, *FEMS Microbiology Letters*, Volume 366, Issue 11, June 2019, fnz135, https://doi.org/10.1093/femsle/fnz135

*Denotes equal contribution

Conference Presentations

---

1. Investigation of the metabolites in ovarian cancer using imaging mass spectrometry, Poster presentation, Chicago Mass Spec Day, July 2019
2. Systematic screening of marine macroorganisms for widespread drug discovery, joint poster presentation, USF Research and Arts Colloquium, April 2016.
3. Finalist, screening of marine macroorganisms for widespread drug discovery, poster presentation, American Institute of Chemical Engineers Southern Regional Conference, University of Alabama, April 2016.
4. Utilization of yeast-based multiplex assay to screen natural products as potential targets for endectocidal drug development, poster presentation, USF Chemistry Departmental Castle Conference, April 2015
5. Utilization of yeast-based multiplex assay to screen natural products as potential targets for endectocidal drug development, poster presentation, USF Oktoberfest Research Presentations, October 2014
6. Honorable mention, Utilization of yeast-based multiplex assay to screen natural products as potential targets for endectocidal drug development, joint poster presentation, USF Chemistry Departmental Castle Conference, April 2014

Teaching Experience

Teaching Assistant, UIC — Spring 2020

College of Pharmacy, PHAR 440: Evidence-Based Medicine

Teaching Assistant, UIC — Fall 2019

College of Pharmacy, PHAR 413: Hospital IPPE

Teaching Assistant, UIC Spring 2019

College of Pharmacy, PHAR 413: Hospital IPPE

Teaching Assistant, UIC Fall 2018

College of Pharmacy, PHAR 504: Immunology/Respiratory

Honors and Awards

1. Poster Session Finalist, American Institute of Chemical Engineers Southern Regional Conference, 2016
2. USF Honors College Student Researcher Award, 2015
3. Honorable Mention, Raymond N. Castle Conference, USF Chemistry Departmental Conference, 2014
4. USF Honors College Discovery Scholar Scholarship recipient, 2014 – 2017
5. USF Presidential Scholarship, 2013 – 2017
6. Girl Scout Gold Award Recipient, 2013

Outreach

Lincoln Park Conservatory Volunteer, October 2018 ongoing.

SACNAS Travel Scholarship Reviewer, May 2019

NSF Outreach trial with the Boys and Girls Club, Jan 2019

Society of Women Engineers, 2014 to 2017. 2016-2017 Outreach Chair.

Give Kids the World Volunteer, 2008 to 2017.